N 63 15509

NASA TN D-1870

TECHNICAL NOTE

D-1870

AN INVESTIGATION OF RESONANT, NONLINEAR, NONPLANAR FREE SURFACE OSCILLATIONS OF A FLUID

By R. E. Hutton

Prepared under Contract NASr-80 by
SPACE TECHNOLOGY LABORATORIES, INC.
Redondo Beach, California
for

NATIONAL AERONAUTICS AND SPACE ADMINISTRATION
WASHINGTON

May 1963

554723

72p

TABLE OF CONTENTS

NATIONAL AERONAUTICS AND SPACE ADMINISTRATION

TECHNICAL NOTE D-1870

AN INVESTIGATION OF RESONANT, NONLINEAR, NONPLANAR FREE SURFACE OSCILLATIONS OF A FLUID*

by R.E. Hutton**

SUMMARY

A theoretical investigation was conducted of the motion of fluid in a tank subjected to lateral harmonic vibration at a frequency in the neighborhood of the lowest resonant frequency of the mass of fluid. The investigation indicates that nonplanar fluid motion is due to a nonlinear coupling between fluid motions parallel and perpendicular to the plane of excitation, and that this coupling takes place through the free surface waves. These theoretical conclusions were experimentally confirmed using a cylindrical tank about 12 inches in diameter and partially filled with water to a depth of about 9 inches. The tank was translated along a diameter at selected frequencies in the immediate neighborhood of the natural frequency of small, free-surface oscillations. Three types of fluid motion were observed: stable planar, stable nonplanar (rotary), and unstable (swirling). In stable planar motion, the fluid moved harmonically with peak wave height and one stationary nodal diameter perpendicular to the direction of excitation. In stable nonplanar motion, the fluid moved harmonically with a constant peak wave height and one nodal diameter that rotated at constant speed around the tank. In unstable

*Motion picture supplement L-770 has been prepared and is available on loan. A request card and a description of the film are included at the back of this document.

**The author wishes to express his appreciation to Professor J. Miles, who acted as a consultant during this study, for his valuable assistance in guiding this work.

motion the fluid never attained a steady-state harmonic response; peak wave height and nodal diameter rotation rate and direction changed constantly.

The frequency regimes of the different types of motion which are possible in the neighborhood of the lowest natural frequency, f_{11}, of small free-surface waves were as follows:

1) Stable planar motion is possible except in a narrow frequency band roughly centered about f_{11}.

2) Stable nonplanar motion is possible in a band bounded below by f_{11}.

3) No stable motion, either planar or nonplanar, is possible in a finite frequency region just below f_{11}.

INTRODUCTION

It has been widely observed that when a container of fluid having a free surface is subjected to a transverse harmonic vibration over some frequency ranges, the fluid does not necessarily respond with steady-state harmonic motion in which there is one stationary nodal diameter perpendicular to the direction of excitation. Rather, a wave may be set up which rotates around the tank harmonically or nonharmonically, even though the forcing motion is harmonic. The rotating wave phenomenon persists over a range of forcing frequencies centered about the natural frequency of small amplitude free surface waves.

Specifically, the behaviour of a free-surface fluid in a container undergoing transverse harmonic vibration of increasing frequency is as follows. When the container is excited at a frequency appreciably below the lowest natural frequency, f_{11}, of small, free-surface oscillations, the steady-state fluid motion is harmonic with a constant peak wave height and a single nodal diameter perpendicular to the direction of excitation. As the excitation frequency is increased, the wave height increases. At a frequency a little less than f_{11}, the nodal diameter

begins to rotate at a nonsteady rate and with a varying peak wave height. This unstable swirling motion persists up to a frequency a little above the natural frequency, where once again the steady-state fluid motion is harmonic with constant peak wave height and a fixed nodal diameter perpendicular to the direction of excitation. An additional increase in excitation frequency from this stable point reduces the wave height until the cycle begins again as the next resonant frequency is approached.[1*]

In addition to harmonic planar motion and nonharmonic swirling motion, there is a third, which in this report is called harmonic nonplanar motion. In the steady state, it is characterized by a constant peak wave height and a single nodal diameter which rotates at a constant rate. Harmonic nonplanar motion occurs in a frequency range bounded below by f_{11}.

According to the linear approximations usually employed, a free surface fluid in a container undergoing transverse harmonic vibration should exhibit a steady-state planar harmonic motion at all frequencies except resonance. The fact that harmonic nonplanar and unstable motions occur has lead investigators[2] to suggest that nonlinear and viscous effects plan an important role. However, no extensive studies have been conducted to resolve this problem. The following work shows that the rotary and swirling motion can be accurately predicted in an inviscid liquid if the analysis includes the appropriate nonlinear effects.

SYMBOLS

a = tank radius

a_n = coefficients in kinematic free-surface condition, Equation (A.5)

a_{mn} = coefficients in kinematic free-surface condition, Equation (A.6)

*Superscript numericals refer to references at the end of this report.

b_{mn} = coefficients in dynamic free surface condition, Equation (A.8)

c_i = amplitude perturbation coefficients, Equation (A.42)

d_{mn} = matrix elements defined in Equation (A.44)

f_n = first slosh mode generalized amplitude coefficients, Equation (A.23)

f_{mn} = natural frequency of the mn'th sloshing mode, cps

g = acceleration of gravity = 386 in/sec

h = fluid depth

$\vec{i}, \vec{j}$ = unit vectors along x, y axes, Figure 1

$\vec{i}_r, \vec{i}_\theta, \vec{i}_z$ = unit vectors along r, θ, z axes, Figure 1

k_n, k_{no} = parameters defined in Equation (A.36)

m, n = integer subscripts referring to the mn'th mode

p_{mn} = natural frequency of the mn'th sloshing mode, rad/sec

$\vec{q}$ = fluid velocity vector

r = fluid particle radial coordinate

t = time

x_1 = tank displacement

$\dot{x}_1$ = tank velocity

A_{mn}, B_{mn} = velocity potential generalized coordinate

$\hat{A}_{mn}, \hat{B}_{mn}, \hat{C}_{mn}, \hat{D}_{mn}$ = velocity potential generalized coordinates, Equation (A.30)

B_n = free-surface boundary condition parameter, Equation (A.12)

F_1 = expansion coefficients defined by Equation (A.38a)

G_n = functions defined by Equation (12)

H = function defined by Equation (13)

$\hat{H}_n$ = parameters defined by Equation (A.36)

I_n = integrals defined by Equation (A.36)

I^n_{qm} = integrals defined by Equations (A.32) and (A.36)

J_m = Bessel function of the first kind of order m

K = parameter defined by Equation (A.36)

K_o = parameters defined by Equation (A.32)

K_{10}, K_{20} = parameters defined by Equation (A.38b)

K_1, K_2 = parameters defined by Equation (A.38a)

K_3, K_4 = parameters defined by Equation (A.41)

M_n = determinants defined by Equation (A.47) and (A.54)

a_{mn} = parameter defined in Equation (A.36)

γ = velocity potential function steady-state amplitude, Equations (A.39a) and (A.40a)

ϵ = tank velocity amplitude

ϵ_o = tank displacement amplitude

ζ = velocity potential function steady-state amplitude, Equation (A.40a)

η = wave height

θ = cylindrical coordinate system coordinate

λ = perturbation parameter in Equation (A.42)

λ_1, λ_2 = roots of perturbation characteristics equation

λ_{mn} = roots of $J'_m(\lambda_{mn} a) = 0$

ν = transformed frequency, Equation (A.19)

τ = transformed time, Equation (A.19)

ϕ_k = k^{th} derivative of velocity potential function evaluation on z = 0, Equation (A.4)

ω = angular forcing frequency of tank motion

Γ = function defined in Equation (A.1)

Φ = total velocity potential function

$\tilde{\Phi}$ = disturbance velocity potential function

Ω_{0n}, Ω_{2n} = parameters defined by Equation (A.31)

x_n, ψ_n = disturbance potential functions defined by (A.18), (A.23) and (A.27a, b)

$$\frac{D}{Dt} \equiv \frac{\partial}{\partial t} + u \frac{\partial}{\partial r} + v \left(\frac{1}{r}\right) \frac{\partial}{\partial \theta} + w \frac{\partial}{\partial z}$$

$$\nabla \equiv \vec{i}_r \frac{\partial}{\partial r} + \vec{i}_\theta \left(\frac{1}{r}\right) \frac{\partial}{\partial \theta} + \vec{i}_z \frac{\partial}{\partial z}$$

$$\nabla^2 \equiv \frac{\partial^2}{\partial r^2} + \left(\frac{1}{r}\right) \frac{\partial}{\partial r} + \left(\frac{1}{r^2}\right) \frac{\partial^2}{\partial \theta^2} + \frac{\partial^2}{\partial z^2}$$

ANALYSIS

The object of this investigation is to determine the response of a fluid contained in a cylindrical tank which is undergoing lateral harmonic vibration in the neighborhood of the lowest natural frequency of small, free surface waves. In this section the main steps in the analytical derivation are presented, with the algebraic details relegated to the appendix.

Figure 1 illustrates the geometry and coordinate system which is used in the analysis. The tank is assumed to be forced in the fixed $x_o z_o$-plane only and this motion is denoted by $x_1(t)$. The r, θ, z coordinate system moves with the tank with the plane z = 0 coinciding with the quiescent free surface.

Throughout the analysis it will be assumed that the fluid is incompressible, inviscid, initially irrotational and that the only body

force is that of gravity, which is oriented along the negative z-axis. Under these assumptions the fluid velocity vector $\vec{q}$ can be written as

$$\vec{q} = \nabla\Phi \tag{1}$$

where the velocity potential function Φ is expressed in terms of the moving coordinates, r, θ, z. If Φ is written as the sum of a disturbance potential function $\tilde{\Phi}$ and a function accounting for the tank motion, i.e.

$$\Phi(r, \theta, z, t) = \dot{x}_1 \, r \cos\theta + \tilde{\Phi}(r, \theta, z, t) \quad , \tag{2}$$

then under the above assumptions the boundary value problem to be considered can be stated as[3]

$$\left.\begin{aligned} &\nabla^2\tilde{\Phi}(r,\ \theta,\ z,\ t) = 0 \quad \text{in} \begin{cases} 0 \le r < a \\ 0 \le \theta \le 2\pi \\ -h < z < \eta \end{cases} \\ &\tilde{\Phi}_z = 0 \qquad\qquad \text{on } z = -h \\ &\tilde{\Phi}_r = \dot{x}_1 \cos\theta \qquad \text{on } r = a \end{aligned}\right\} \tag{3}$$

and

$$g\eta + \tilde{\Phi}_t + \frac{1}{2}(\nabla\tilde{\Phi} \cdot \nabla\tilde{\Phi}) = -\ddot{x}_1 \, r \cos\theta \text{ on } z = \eta, \tag{4}$$

$$\eta_t + \tilde{\Phi}_r\eta_r + \frac{1}{r^2}\tilde{\Phi}_\theta\eta_\theta = \tilde{\Phi}_z \text{ on } z = \eta \ . \tag{5}$$

The dots above x_1 represent time derivatives and the subscripts t, r, θ, and z respectively. The first equation of (3) requires that the disturbance velocity potential function satisfy Laplace's equation which is a linear partial differential equation. The dynamic condition, Equation (4), is Bernoulli's equation with the pressure set equal to zero on the free surface $z = \eta$. The kinematic condition, Equation (5), is simply a statement that a fluid particle on the free surface has the same vertical velocity as the free surface.

It is to be noted that the only nonlinear character of this boundary value problem enters through the free-surface boundary conditions on $z = \eta$. In a linear analysis, the nonlinear terms in Equation (4) and (5) are neglected under the assumption that the wave height and fluid velocities are small, and then, these linerized free-surface conditions are satisfied on the undisturbed free surface $z = 0$. However, when the tank is driven at or near the lowest resonant frequency f_{11}, the wave height and fluid velocities are not small, and it is essential that the nonlinear terms in Equation (4) and (5) be taken into account.

Since the free surface $z = \eta$ is an unknown in the problem, the free-surface boundary conditions are combined in the appendix into one boundary condition in which the wave height η has been eliminated. Thus, the boundary value problem to be considered can be restated as:

$$\left.\begin{aligned} \nabla^2 \tilde{\Phi}(r,\theta,z,t) &= 0 \quad \text{in} \quad \begin{cases} 0 \leq r < a \\ 0 \leq \theta \leq 2\pi \\ -h < z < \eta \end{cases} \\ \tilde{\Phi}_z &= 0 \quad \text{on} \quad z = -h \\ \tilde{\Phi}_r &= 0 \quad \text{on} \quad r = a \end{aligned}\right\} \tag{6}$$

and

$$B_1 + B_2 + B_3 + O(\eta^4) = 0 \tag{7}$$

where the terms B_1. B_2, B_3, defined in the appendix, depend only upon the velocity potential function $\tilde{\Phi}$ and its derivaties, all evaluated on the undisturbed free-surface $z = 0$, and also upon the prescribed tank displacement $x_1(t)$. The tank displacement is taken as

$$x_1(t) = \epsilon_o \sin\omega t$$

with ϵ_o "small" and ω close to or equal to the lowest sloshing natural frequency p_{11}. A steady state harmonic solution to boundary value problem (6) and (7) is posed in the form

$$\Phi = \epsilon^{1/3}\left[\psi_1(\vec{r}, t)\cos\omega t + x_1(\vec{r}, t)\sin\omega t\right] + \epsilon^{2/3}\left[\psi_o(\vec{r}) + \psi_2(\vec{r})\cos 2\omega t + x_2(\vec{r})\sin 2\omega t\right] + \epsilon\left[\psi_3(\vec{r})\cos 3\omega t + x_3(\vec{r})\sin 3\omega t\right] \quad (8)$$

where $\epsilon = \omega\epsilon_o$ is the peak tank velocity and the functions x_n, ψ_n satisfy (6) identically with only ψ_1 and x_1 depending upon time. The notation $\vec{r}$ means dependence upon r, θ, and z. A set of normal sloshing modes which satisfies (6) exactly is

$$\left[A_{mn}(t)\cos m\theta + B_{mn}(t)\sin m\theta\right] J_m(\lambda_{mn} r)\frac{\cosh\left[\lambda_{mn}(z+h)\right]}{\left[\cosh\lambda_{mn} h\right]}$$

where the J_m are Bessel functions of the first kind and of order $m = 0, 1, 2, \cdots$, and λ_{mn} are an infinite set of numbers for each m obtained from the zeros of $J'_m(\lambda_{mn} a)$. The functions $A_{mn}(t)$ and $B_{mn}(t)$ depend only upon time and are called the generalized coordinates of the mn'th mode. The natural frequency of small, free-surface oscillations in the mn'th mode is denoted by p_{mn}. In this problem, in which the tank is harmonically translated at a frequency close to or at the lowest natural frequency associated with the J_1 mode, p_{11}, the generalized coordinates A_{11} and B_{11} dominate all other generalized coordinates. For this reason, the first order terms of (8) contain the first J_1 mode only and x_1 and ψ_1 are taken in the appendix as

$$\left.\begin{aligned} \psi_1 &= \left[f_1(r)\cos\theta + f_3(r)\sin\theta\right] J_1(\lambda_{11} r)\frac{\cosh\left[\lambda_{11}(z+h)\right]}{\cosh\left[\lambda_{11}h\right]} \\ x_1 &= \left[f_2(t)\cos\theta + f_4(t)\sin\theta\right] J_1(\lambda_{11} r)\frac{\cosh\left[\lambda_{11}(z+h)\right]}{\cosh\left[\lambda_{11}h\right]} \end{aligned}\right\} \qquad (9)$$

where the transformation

$$\tau = \frac{1}{2}\epsilon^{2/3}\omega t \quad , \quad p_{11}^2 = \omega^2\left[1 - \nu\epsilon^{2/3}\right] \qquad (10)$$

has been introduced. The functions ψ_2 and x_2 depend upon the modes corresponding to J_o and J_2 only and their definitions are given in the appendix.

In the appendix the trial solution (8) is introduced into the free-surface conditon (7) and the terms of which $\epsilon^{1/3}$, $\epsilon^{2/3}$, and ϵ are the coefficients are set equal to zero. The term of which $\epsilon^{1/3}$ is the coefficient depends upon the first J_1 mode only and vanishes identically. The term of which $\epsilon^{2/3}$ is the coefficient depends upon the generalized coordinate of the first J_1 mode and the infinite set of generalized coordinates of the J_o and J_2 modes. With Fourier-Bessel techniques, this equation is satisfied by expressing the generalized coordinates of J_o and J_2 modes in terms of the J_1 mode generalized coordinates. The term of which ϵ is the coefficient depends upon the first J_1 mode and coupling between the J_1 mode and J_o and J_2 modes.

The generalized coordinates of the J_o and J_2 modes are eliminated from the last equation by using the relations (obtained by setting equal to zero, the term of which $\epsilon^{2/3}$ is the coefficient) between the generalized coordinates of the J_1 mode and the J_o and J_2 modes. The resulting equation depends only upon the first J_1 mode generalized coordinates. Next, the equation is satisfied in a Rayleigh-Ritz sense. That is, the equation is first multiplied by $J_1 \cos\theta\, r\, dr\, d\theta$ and integrated over the free surface and is then multiplied by $J_1 \sin\theta\, r\, dr\, d\theta$ and again integrated over the free surface.

Both of these integrated equations have $\sin\omega t$ and $\cos\omega t$ terms. Requiring that the coefficients of each of the $\sin\omega t$ and $\cos\omega t$ terms vanish in both of these two integrated equations gives the nonlinear differential equations that the generalized coordinates f_1, f_2, f_3, f_4, of the first J_1 mode must satisfy. This set of first order differential equations can be written in a compact form using Cartesian tensor summations and writing:

$$\frac{df_i}{d\tau} = G_i(f_1, f_2, f_3, f_4) \quad , \quad i = 1, 2, 3, 4 \tag{11}$$

where

$$\left.\begin{aligned} G_1 &= -H,_2 \quad , \quad G_3 = -H,_4 \\ G_2 &= H,_1 \quad , \quad G_4 = H,_3 \end{aligned}\right\} \tag{12}$$

and

$$H = F_1 f_1 + \frac{1}{2}\nu f_{jj} + \frac{1}{4}K_1(f_j f_j)^2 - \frac{1}{2}K_2(f_2 f_3 - f_1 f_4)^2 \tag{13}$$

Subscripts following commas imply differentiation with respect to the corresponding f_j and repeated subscripts imply summation. The constants F_1, K_1, K_2, which depend upon tank geometry only, are defined in the appendix. A steady state harmonic solution of the boundary value problem expresed in Equations (6) and (7) corresponds to the zeros of the four equations indicated in (11). In the appendix it is found that there are two such solutions. The first is called planar motion and the solution is given by

$$f_1 = \gamma \quad ; \quad f_2 = f_3 = f_4 = 0 \tag{14a}$$

with

$$\nu = -F_1\gamma^{-1} - K_1\gamma^2 \quad . \tag{14b}$$

The second is called nonplanar motion and the solution is given by

$$f_1 = \gamma \quad , \quad f_2 = f_3 = 0 \quad , \quad f_4^2 = b^2 = \gamma^2 + \frac{F_1}{K_2}\,\gamma^{-1} \tag{15a}$$

with

$$\nu = -K_3\gamma^{-1} + K_4\gamma^2 \quad . \tag{15b}$$

The constants K_3 and K_4 are also defined in the appendix. In the appendix these two solutions are examined to determine whether they are stable by imposing a slight perturbation from the steady state solution and investigating the subsequent motion. If the subsequent motion increases with time following the perturbation, the solution is called unstable. The analytical investigation of stability is carried out in the appendix, wherein the perturbation

$$f_i(\tau) = f_i^{(0)} + c_i\, e^{\lambda\tau} \tag{16}$$

is imposed. The $f_i^{(0)}$ denote the steady state solution given by (14) and (15) with the disturbance c_i assumed small. Introducing (16) into the set (11) leads to an algebraic equation in λ. Any root λ of this equation with a positive real part indicates a motion that grows with time and the corresponding solution is called unstable. It is found that the solutions given by (14) and (15) are stable only over certain ranges of transformed forcing frequency ν. Figure 2 summarizes the regions of stable and unstable planar motion. From the figure it is noted that the theory predicts that planar motion is not stable over a frequency band centered about $\nu = 0$ (or $\omega = p_{11}$).

NUMERICAL EXAMPLE

The following numerical calculations are based on the theoretical results for the parameters corresponding to the sloshing tests, which are

$$a = \text{tank radius} = 5.938 \text{ inches} ,$$

$$h = \text{water depth} = 8.907 \text{ inches} .$$

With the values $\lambda_{11}a = 1.84119$ and $J_1(\lambda_{11}a) = 0.581865$, Equations (A.24) and A.38a) are evaluated to be

$$F_1 = 8.53992 , \quad \alpha_{11} = 0.99205$$

and

$$p_{11} = 10.897 \text{ rad/sec} = 1.734 \text{ cps} .$$

In the evaluation of the coefficients K_1 and K_2 the infinite series terms in Equations (A.35a, b) are approximated by their first five terms. To indicate what errors this finite series approximation might cause, the following facts are cited. In the calculations of $\hat{G}_1$ and $\hat{G}_2$, which contribute to K_1 and K_2, the last three terms were only about 1 percent of the first two terms.

The Bessel function parameters required to sum the finite series obtained from Reference 4 are presented in Table 1.

The values in Table 1 are used to compute the quantities defined by Equations (A.31), (A.32), (A.36), and (A.38a, b). The results are presented in Table 2.

The amplitude-frequency relation for the planar motion is

$$\nu = -F_1\gamma^{-1} - K_1\gamma^2 = -8.5399\gamma^{-1} - 0.48528 \times 10^{-5}\gamma^2. \qquad (17)$$

The lower limit boundaries between stable and unstable motions are computed from Equations (A.49a, b)

$$\left.\begin{aligned} \gamma &= \left(\frac{F_1}{2K_1}\right)^{1/3} = 95.82 \\ \text{and} \\ \nu &= -3K_1\left(\frac{F_1}{2K_1}\right)^{2/3} = -0.1337 \ , \end{aligned}\right\} \tag{18}$$

The upper limit boundaries are computed from Equation (A.50a, b):

$$\left.\begin{aligned} \gamma &= -\left(\frac{F_1}{K_2}\right)^{1/3} = -85.41 \\ \text{and} \\ \nu &= (K_2 - K_1)\left(\frac{F_1}{K_2}\right)^{2/3} = 0.06459 \ . \end{aligned}\right\} \tag{19}$$

The amplitude-frequency relation for the nonplanar motion is

$$\nu = -K_3\gamma^{-1} + K_4\gamma^2 = -3.0235\gamma^{-1} + 4.0010 \times 10^{-6}\gamma^2 \tag{20}$$

and

$$\zeta^2 = \gamma^2 + \frac{F_1}{K_2}\gamma^{-1} = \gamma^2 + 6.2305 \times 10^5\gamma^{-1} \ . \tag{21}$$

Stability of the steady-state nonplanar solution is determined by examining the roots of Equation (A.53), namely:

$$\lambda^4 + (M_3 + M_4)\lambda^2 + M_5M_6 = 0 \ , \qquad (22)$$

where the coefficients are obtained from (A.56) and are found to be

$$M_3 + M_4 = 4K_2^2\gamma\left(\gamma^3 + \frac{3K_2 - 2K_1}{4K_2^2} F_1\right)$$

$$= 7.5148 \times 10^{-10}\gamma(\gamma^3 + 3.5699 \times 10^5) \ ,$$

$$M_5M_6 = 4K_2^2(K_2 - 2K_1)F_1\gamma^{-1}\left(\gamma^3 + \frac{F_1}{K_2}\right)\left[\gamma^3 + \frac{K_1F_1}{2K_2(K_2 - 2K_1)}\right]$$

$$= 2.5677 \times 10^{-9}\,\gamma^{-1}(\gamma^3 + 6.2305 \times 10^5)(\gamma^3 + 3.7784 \times 10^5). \qquad (23)$$

Stability calculations for the nonplanar motion are summarized in Table 3.

The computed results for this numerical example are presented in Figures 3 through 8. Figure 3 is a plot of Equation (17) showing the relation between γ and ν for the harmonic planar motion and indicating the corresponding ranges of stable and unstable motion. Figure 4 is a plot of Equation (20), showing the relation between γ and ν for the harmonic nonplanar motion; the ranges of stable and unstable motion are indicated, as well as the range in which the solution is imaginary. In Figure 5, the plot of ζ versus ν for this same nonplanar motion is derived from Equations (20) and (21). Figure 6 is a plot of γ versus ν, showing only the stable branches of Figures 3 and 4. Figure 7 shows the unstable regions for both the planar and nonplanar motions as functions of the peak tank velocity, ϵ, and the tank displacement frequency, $\omega/2\pi$. These curves are computed from the transformation equation

$$p_{11}^2 = \omega^2(1 - \nu_\epsilon^{2/3}) \tag{24}$$

for the value of $p_{11} = 10.897$ rad/sec $= 1.734$ cps. An evaluation of Equation (24) requires the limiting values of ν. The limits of ν separating stable and unstable regions for the planar motion are shown in Figure 3 and are given in Equations (18) and (19) as $\nu = -0.1337$ and $\nu = 0.06459$. The value of ν separating stable and unstable regions for the only stable nonplanar motion, which is for $\gamma > 0$, is shown in Figure 4 and is tabulated in Table 3 as $\nu = -0.03027$. Substituting these values into Equation (24) and solving for ϵ as a function of $\omega/2\pi$ provides the data used to plot the curves in Figure 7. Figure 8 is a plot of the approximate planar motion stability boundary as a function of the dimensionless ratios f/f_{11} and ϵ_o/a. These curves approximate the stability boundary for a tank in which the fluid depth is greater than the tank radius, in which case, the stability boundary is nearly independent of the fluid depth. The expressions used to construct this figure were developed in the following manner: First by referring to Equations (A.36), (A.38a, b), (A.49b) and (A.50b) it is noted that the instability limits are approximately proportional to $(ga)^{-1/3}$. That is

$$\nu_u = -3K_1\left(\frac{F_1}{2K_1}\right)^{2/3} \propto g^{-1}a^{-3}\left(\frac{a}{g^{-1}a^{-3}}\right)^{2/3} = (ga)^{-1/3}$$

$$\nu_\ell = (K_2 - K_1)\left(\frac{F_1}{2K_1}\right)^{2/3} \propto (ga)^{-1/3}$$

or, introducing the proportionality constants c_u and c_e gives

$$\nu_u = c_u(ga)^{-1/3} \quad \text{and} \quad \nu_\ell = c_\ell(ga)^{-1/3}$$

For $a = 5.938$ and $g = 386$ the upper and lower stability limits are found to be $\nu_u = -0.1337$ and $\nu_\ell = 0.06459$ so that c_u and c_ℓ become

$$c_u = 0.852 \quad , \quad c_\ell = -1.764 \ .$$

Using Equation (A.19) the ratios of driving frequency to the lowest natural sloshing frequency can be written

$$\left(\frac{f}{f_{11}}\right)^2 = \frac{1}{1 - \nu\epsilon^{2/3}} \approx 1 + \nu\epsilon^{2/3}$$

for $\nu\epsilon^{2/3} << 1$. Since

$$\nu\epsilon^{2/3} \quad \propto \quad (ga)^{-1/3}\left(\omega^2 \epsilon_o^2\right)^{1/3} \approx \left(\frac{p_{11}^2 \epsilon_o^2}{ga}\right)^{1/3} \approx \left[(1.84119)\left(\frac{\epsilon_o^2}{a^2}\right)\right]^{1/3}$$

the upper and lower stability limits can be approximated by the expressions

$$\left.\begin{aligned}\left(\frac{f_u}{f_{11}}\right)^2 &= 1 + 1.04\left(\frac{\epsilon_o}{a}\right)^{2/3} \\ \left(\frac{f_\ell}{f_{11}}\right)^2 &= 1 - 2.16\left(\frac{\epsilon_o}{a}\right)^{2/3}\end{aligned}\right\} \qquad (25)$$

These were the equations used to develop Figure 8.

Experimental Results and Comparison with Theoretical Predictions

The sloshing tests for verification of the theoretical work of this investigation were conducted in the Space Technology Laboratories slosh test facility, shown in Figure 9. This facility consists of a rigid, lightweight tank platform supported so as to allow only a single translation degree of freedom. This is accomplished by long, flexure-ended positioning struts oriented to eliminate rotation about any axis and to make negligible any translation other than that along the lateral drive axis. This design results in a very rigid platform possessing a high resonant frequency compared with the slosh frequency being investigated. The drive mechanism and its platform are also very rigid.

The sinusoidal lateral oscillation of the slosh-tank platform is accomplished with a scotch-yoke mechanism connected to a heavy, variable-speed drive. The amount of eccentricity of the drive stud can be preset to produce a peak-to-peak stroke length up to 1 inch. While the drive motor is running, the drive stud can be moved rapidly from center (no stroke) to preset stroke position to start lateral excitation. Thus, the amount of excitation can be varied at any selected frequency.

A cylindrical tank about 12 inches in diameter, partially filled with water to a depth of about 9 inches, was used for the tests. Testing was conducted in the following manner. The amplitude of tank motion, ϵ_o, was set and was left constant for the entire test. Then the tank was driven at a desired frequency and when steady-state conditions appeared to be established, the frequency and wave height were read and the fluid behavior noted.

The driving frequency was measured by sensing the rotational speed of the scotch-yoke drive and recording this speed on a Berkeley freqeuncy meter. The tank peak-to-peak amplitude ($2\epsilon_o$) was measured by placing a dial indicator beside the tank in the plane of tank motion and observing the extreme positions of the dial indicator needle. The wave height was measured by reading a 6-inch scale (graduated in hundredths of an inch) attached to the plexiglas tank in the plane of the tank motion and zeroed on the quiescent water level. The error of the three measurements is estimated to be as follows: drive frequency, $\omega/2\pi = \pm 0.004$ cps; tank amplitude, $\epsilon_o = \pm 0.0005$ inch; wave height was more difficult to read and the probable wave height error was ± 0.2 inch.)

Three types of fluid motion were noted: stable planar, stable nonplanar, and unstable. Stable planar motion is a steady-state fluid motion with a constant peak wave height and a stationary single nodal diameter perpendicular to the direction of excitation. Stable nonplanar motion is a steady-state rotary fluid motion with a constant peak wave

height and a single nodal diameter that rotates at a constant speed. This motion has the appearance of a surface wave traveling around the tank at a constant speed and in a single direction. Unstable motion is a swirling fluid motion that never attains a steady-state harmonic response; the peak wave height and nodal diameter rotation rate and direction continually change with time. The surface wave in unstable motion may build up and then decay; it may rotate first in one direction, then stop, and rotate the other way. At times, the wave may slosh for several cycles in a plane perpendicular to the plane in which the tank is being driven, then rotate around and slosh in the driven plane for several cycles.

To locate the limits of the planar motion instability region, the first test reading was made at a frequency in the stable region well below the instability region. After the first reading was recorded the driving frequency was increased. When steady-state motions were again established, the wave height and fluid behavior were again recorded. This process was continued until the frequency was raised to the point where planar motion became unstable, indicating the lower limit of the unstable planar region. With this boundary established, the driving frequency was increased above the natural frequency to a frequency in the upper stable planar region, and the steady-state wave height was recorded. This process was repeated, reducing the frequency each time, until the upper limit of the unstable region was located.

After the planar motion exploration was completed, the stable nonplanar motion was investigated. This motion occurred primarily above the natural frequency and overlapped a frequency range in which stable planar motions had been observed.

To verify further that both planar and nonplanar motions could be stable within a common frequency range, the following test was carried out. With the fluid at rest, the tank motion was started. When a steady-state condition at a selected frequency was reached the fluid

was observed to assume stable planar motion. While the water maintained this stable motion, a paddle was inserted into the tank and the motion was deliberately perturbed into a random behavior. When the paddle was removed, the water motion sometimes settled back into the original planar mode, and at other time became nonplanar. Observations of the latter cases indicated that this nonplanar mode was indeed a stable motion which would continue until the driving motion was changed. This test thus demonstrated that both stable motions were possible at a single driving frequency. A possible conclusion from several repetitions of this experiment is that the nonplanar mode requires the addition of energy into the system.

Additional testing verified the existence of a finite region of unstable motion below the natural frequency. In this region, no stable harmonic steady-state motions were found.

The data taken during these tests are summarized in Figures 10, 11, and 12. Figure 10 is a plot of faired curves through the observed planar motion peak wave height data for various tank driving frequencies. Figure 11 shows a faired curve through the test data of the nonplanar motion peak wave height for a driving amplitude of 0.032 inches. Figure 12 is a plot of the data of Figure 10 when the frequency is transformed by the equation

$$\nu = \left(1 - \frac{p_{11}^2}{\omega^2}\right)\epsilon^{-2/3}$$

and the wave height is divided by $\epsilon^{1/3}$. This scaling was suggested by the theoretical investigation.

In Figure 13, the predicted stable and unstable planar and nonplanar regions of Figure 7 are compared with the test data. Figure 13 indicates that the predicted boundaries of the instability region agree closely with the experiment for small values of ϵ. Poorer agreement

for the nonplanar motion stability boundary is not surprising because of the difficulty of visually detecting the point at which the fluid motion changes character; as the frequency is decreased, the transition is gradual from the steady-state harmonic nonplanar motion to the non-harmonic nonplanar motion existing in the instability region.

CONCLUSIONS

This investigation has attempted to provide an explanation for the motion of fluid in a partially filled tank when the tank is laterally vibrated over a frequency range centered at the lowest natural frequency of small free-surface oscillations. The theoretical studies outlined herein predicted the forcing frequency ranges on which there were stable steady-state harmonic planar and nonplanar fluid responses and the range of frequencies in which no harmonic motions are stable. These studies have shown that the mechanism that causes the swirling fluid motion in the unstable regime and the rotary harmonic motion in the nonplanar regime is a nonlinear coupling of fluid motions parallel with and perpendicular to the excitation plane. It is evident that this nonlinear coupling takes place through the free-surface waves and the observed fluid behavior can be predicted only if the higher-order terms in the free-surface dynamic and kinematic boundary conditions are included in the analysis.

Space Technology Laboratories, Inc.
Redondo Beach, California, November 1, 1962

APPENDIX

1. Free Surface Boundary Condition

Since the free-surface height η is an unknown in the problem, it is desirable to replace the two free-surface conditions (4) and (5) by one equation that does not contain η. First, it will be convenient to eliminate the partial derivatives of η occurring in Equation (5) by use of Equation (4). Now, Equation (4) is of the form

$$-g\eta = \Gamma\left[r, \theta, \eta(r, \theta, t), t\right] = \tilde{\Phi}_t + \frac{1}{2}\left(\tilde{\Phi}_r^2 + \frac{1}{r^2}\tilde{\Phi}_\theta^2 + \tilde{\Phi}_z^2\right) + \ddot{x}_1 r\cos\theta \quad , \text{(A.1)}$$

so that η is no longer an independent variable. Thus, the partial derivatives η_t, η_r, η_θ to be obtained from Equation (A.1) must reflect the fact that Γ also depends upon r, θ, and t through the free-surface parameter η. From Equation (A.1) it is determined that

$$\begin{aligned} -g\eta_t &= \Gamma_t + \Gamma_\eta \eta_t \quad , \\ -g\eta_r &= \Gamma_r + \Gamma_\eta \eta_r \quad , \\ -g\eta_\theta &= \Gamma_\theta + \Gamma_\eta \eta_\theta \quad , \end{aligned}$$

or

$$\left.\begin{aligned} -(g+\Gamma\eta)\eta_t &= \Gamma_t = \tilde{\Phi}_{tt} + \tilde{\Phi}_r\tilde{\Phi}_{rt} + \frac{1}{r^2}\tilde{\Phi}_\theta\tilde{\Phi}_{\theta t} + \tilde{\Phi}_z\tilde{\Phi}_{zt} + \dddot{x}_1 r\cos\theta \quad , \\ -(g+\Gamma\eta)\eta_r &= \Gamma_r = \tilde{\Phi}_{rt} + \tilde{\Phi}_r\tilde{\Phi}_{rr} - \frac{1}{r^3}\tilde{\Phi}_\theta^2 + \frac{1}{r^2}\tilde{\Phi}_\theta\tilde{\Phi}_{\theta r} + \tilde{\Phi}_z\tilde{\Phi}_{zr} + \ddot{x}_1\cos\theta, \\ -(g+\Gamma\eta)\eta_\theta &= \Gamma_\theta = \tilde{\Phi}_{\theta t} + \tilde{\Phi}_r\tilde{\Phi}_{r\theta} + \frac{1}{r^2}\tilde{\Phi}_\theta\tilde{\Phi}_{\theta\theta} + \tilde{\Phi}_z\tilde{\Phi}_{\theta z} - \ddot{x}_1 r\sin\theta \quad , \end{aligned}\right\} \text{(A.2)}$$

where

$$\Gamma_\eta = \tilde{\Phi}_{\eta t} + \tilde{\Phi}_r \tilde{\Phi}_{r\eta} + \frac{1}{r^2}\tilde{\Phi}_\theta \tilde{\Phi}_{\theta\eta} + \tilde{\Phi}_z \tilde{\Phi}_{\eta z} \ .$$

Since Γ_η is equal to Γ_z for $z = \eta$,

$$\Gamma_\eta = \Gamma_z = \tilde{\Phi}_{zt} + \tilde{\Phi}_r \tilde{\Phi}_{rz} + \frac{1}{r^2}\tilde{\Phi}_\theta \tilde{\Phi}_{\theta z} + \tilde{\Phi}_z \tilde{\Phi}_{zz} \ .$$

If Equation (5) is multiplied by $-(g + \Gamma_\eta)$ and Equations (A.2) are used, Equation (5) reduces to

$$\tilde{\Phi}_{tt} + g\tilde{\Phi}_z + 2\tilde{\Phi}_r \tilde{\Phi}_{rt} + \frac{2}{r^2}\tilde{\Phi}_\theta \tilde{\Phi}_{\theta t} + 2\tilde{\Phi}_z \tilde{\Phi}_{zt} + \tilde{\Phi}_r{}^2 \tilde{\Phi}_{rr} + \tilde{\Phi}_z{}^2 \tilde{\Phi}_{zz}$$

$$+\frac{1}{r^4}\tilde{\Phi}_\theta{}^2 \tilde{\Phi}_{\theta\theta} - \frac{1}{r^3}\tilde{\Phi}_r \tilde{\Phi}_\theta^2 + \frac{2}{r^2}\tilde{\Phi}_r \tilde{\Phi}_\theta \tilde{\Phi}_{r\theta} + \frac{2}{r^2}\tilde{\Phi}_z \tilde{\Phi}_\theta \tilde{\Phi}_{\theta z} + 2\tilde{\Phi}_r \tilde{\Phi}_z \tilde{\Phi}_{rz}$$

$$= - \dddot{x}_1 r \cos\theta + \ddot{x}_1 \left(\frac{1}{r}\tilde{\Phi}_\theta \sin\theta - \tilde{\Phi}_r \cos\theta\right) ,$$

on $z = \eta$. (A.3)

Since the potential functions must be evaluated on $z = \eta$, Equation (A.3) depends upon η implicitly and Equation (4) depends upon η both implicitly and explicitly. Now the wave height η can be eliminated between Equations (4) and (A.3), if these two equations are first expanded in a Taylor series in η about $z = 0$. By introducing the notation

$$\phi_k \equiv \tilde{\Phi}_k(r, \theta, z = 0, t) \ , \qquad (A.4)$$

where the subscript k represents any order of partial differentiation, the Taylor series expansions for Equations (A.3) and (4) can be written in the forms

$$a_0 + a_1\eta + a_2\eta^2 + a_3\eta^3 + \ldots = 0 \tag{A.5}$$

and

$$b_0 + b_1\eta + b_2\eta^2 + b_3\eta^3 + \ldots = 0 \ , \tag{A.6}$$

respectively, where

$$\left.\begin{aligned} a_0 &= a_{00} + a_{01} + a_{02} \ , \quad b_0 = b_{00} + b_{01} \ ; \\ a_1 &= a_{11} + a_{12} + a_{13} \ , \quad b_1 = g + b_{11} + b_{12} \ ; \\ a_2 &= a_{22} + a_{23} + a_{24} \ , \quad b_2 = b_{22} + b_{23} \ ; \\ &\ldots \qquad\qquad\qquad \ldots \end{aligned}\right\} \ . \tag{A.7}$$

and where

$$\left.\begin{aligned} a_{00} &= \phi_{tt} + g\phi_z + r\ddot{x}_1 \cos\theta \ , \\ a_{01} &= 2\phi_r\phi_{rt} + \frac{2}{r^2}\phi_\theta\phi_{\theta t} + 2\phi_z\phi_{zt} + \ddot{x}_1\left(\phi_r \cos\theta - \frac{1}{r}\phi_\theta \sin\theta\right) , \\ a_{02} &= \phi_r{}^2\phi_{rr} + \frac{1}{r^4}\phi_\theta{}^2\phi_{\theta\theta} + \phi_z{}^2\phi_{zz} - \frac{1}{r^3}\phi_r\phi_\theta{}^2 + 2\phi_r\phi_z\phi_{rz} \\ &\quad + \frac{2}{r^2}\phi_r\phi_\theta\phi_{r\theta} + \frac{2}{r^2}\phi_z\phi_\theta\phi_{\theta z} \ , \\ a_{11} &= \phi_{ttz} + g\phi_{zz} \ , \quad a_{22} = \frac{1}{2}(\phi_{ttzz} + g\phi_{zzz}) \ , \\ a_{12} &= 2\left(\phi_{rz}\phi_{rt} + \phi_r\phi_{rzt} + \frac{1}{r^2}\phi_{\theta z}\phi_{\theta t} + \frac{1}{r^2}\phi_\theta\phi_{\theta zt} + \phi_{zz}\phi_{zt} \right. \\ &\quad \left. + \phi_z\phi_{zzt}\right) + \ddot{x}_1\left(\phi_{rz}\cos\theta - \frac{1}{r}\phi_{\theta z}\sin\theta\right) , \\ b_{00} &= \phi_t + r\ddot{x}_1\cos\theta \ , \quad b_{11} = \phi_{tz} \ , \quad b_{22} = \frac{1}{2}\phi_{tzz} \ , \\ b_{01} &= \frac{1}{2}\left(\phi_r{}^2 + \frac{1}{r^2}\phi_\theta{}^2 + \phi_z{}^2\right) , \\ b_{12} &= \phi_r\phi_{rz} + \frac{1}{r^2}\phi_\theta\phi_{\theta z} + \phi_z\phi_{zz} \\ a_{m+1,n+1} &= \frac{1}{(m+1)!}\frac{\partial a_{mn}}{\partial z} \ , \quad b_{m+1,n+1} = \frac{1}{(m+1)!}\frac{\partial b_{mn}}{\partial z} \ . \end{aligned}\right\} \tag{A.8}$$

From Equations (A.6) and (A.7), it is evident that the potential functions are the same order as the wave height. This is readily seen by neglecting the products of η and ϕ in Equation (A.6); then, the first approximation becomes

$$b_{00} + g\eta \doteqdot 0$$

or

$$\eta \doteqdot -\frac{1}{g}\phi_t \ . \tag{A.9}$$

Hence, a term such as $b_2\eta^2$ in Equation (A.6) is of order η^3. Solving Equation (A.6) for η yields

$$\eta = -\frac{b_0}{b_1} - \frac{b_2}{b_1}\eta^2 - \ldots = -\frac{b_0}{b_1} + 0(\eta^3) \ , \tag{A.10}$$

and upon substituting Equation (A.10) into (A.5), the result becomes

$$a_0 + a_1\left[-\frac{b_0}{b_1} + 0(\eta^3)\right] + a_2\left[-\frac{b_0}{b_1} + 0(\eta^3)\right]^2 + 0(\eta^4) = 0 \ ,$$

or

$$a_0 - \frac{a_1 b_0}{b_1} + a_2\frac{b_0^2}{b_1^2} + 0(\eta^4) = 0 \ . \tag{A.11}$$

Now,

$$\frac{a_1 b_0}{b_1} = \frac{(a_{11} + a_{12} + a_{13})(b_{00} + b_{01})}{g + b_{11} + b_{12}}$$

$$= \left(\frac{a_{11}b_{00}}{g}\right) + \left(\frac{a_{11}b_{01} + a_{12}b_{00}}{g} - \frac{a_{11}b_{00}b_{11}}{g^2}\right) + 0(\eta^4)$$

and

$$\frac{a_2 b_0^2}{b_1^2} = \frac{(a_{22} + a_{23} + a_{24})(b_{00} + b_{01})^2}{(g + b_{11} + b_{12})^2} = \left(\frac{a_{22} b_{00}^2}{g^2}\right) + 0(\eta^4) \ ,$$

so that Equation (A.11) becomes

$$B_1 + B_2 + B_3 + 0(\eta^4) = 0 \ , \tag{A.12}$$

where

$$\left.\begin{aligned} B_1 &= a_{00} \ , \\ B_2 &= a_{01} - \frac{a_{11} b_{00}}{g} \ , \\ B_3 &= a_{02} - \frac{a_{11} b_{01} + a_{12} b_{00}}{g} + \frac{a_{11} b_{00} b_{11} + a_{22} b_{00}^2}{g^2} \ . \end{aligned}\right\} \tag{A.13}$$

In summary, the problem statement in terms of disturbance potential functions with the higher-order approximation for the free-surface condition becomes

$$\left.\begin{aligned} &\nabla^2 \tilde{\Phi}(r, \theta, z, t) = 0 \quad \text{in} \begin{cases} 0 \le r < a \\ 0 \le \theta \le 2\pi \\ -h < z < \eta \end{cases} \ , \\ &\tilde{\Phi}_z = 0 \ \text{ on } \ z = -h \ , \\ &\tilde{\Phi}_r = 0 \ \text{ on } \ r = a \ , \end{aligned}\right\} \tag{A.14}$$

$$B_1 + B_2 + B_3 + 0(\eta^4) = 0 \quad \text{on} \quad z = 0 \ , \tag{A.15}$$

2. Steady-State Harmonic Solution

In this section, a steady-state solution to boundary value problem [Equations (A.14) and (A.15)] is derived for the case where the tank displacement motion is

$$x_1 = \epsilon_o \sin \omega t \tag{A.16}$$

and the tank velocity is

$$\dot{x}_1 = \epsilon \cos \omega t \quad , \quad \epsilon = \omega \epsilon_o \tag{A.17}$$

The solution, which is limited to the case where ϵ is small and the driving frequency ω is close to or equal to the first slosh mode frequency p_{11}, is posed in the form*

$$\begin{aligned} \tilde{\Phi} = {} & \epsilon^{1/3} \left[\psi_1(\vec{r}, \tau) \cos \omega t + x_1(\vec{r}, \tau) \sin \omega t \right] \\ & + \epsilon^{1/3} \left[\psi_o(\vec{r}) + \psi_2(\vec{r}) \cos 2\omega t + x_2(\vec{r}) \sin 2\omega t \right] \\ & + \epsilon \left[\psi_3(\vec{r}) \cos 3\omega t + x_3(\vec{r}) \sin 3\omega t \right] , \end{aligned} \tag{A.18}$$

*In the preliminary efforts to find a solution that was valid through third order terms, a solution which included only the J_1 modes was first posed. This, of course, is sufficiently general to obtain an exact solution for the linear problem, but is not adequate for the nonlinear problem. This work clearly showed that the fluid problem is related to the Duffing problem, in that two second order differential equations to be satisfied by the generalized coordinate A_{11} and B_{11} were of the Duffing type and might be described as Duffing's equations generalized to two dimensions. However, more importantly, this work demonstrated that other J_m modes are excited through nonlinear coupling of the free-surface waves. This coupling involved a coupling between the J_1 modes and the other J_m modes that started with third-order terms (only J_o and J_2). It was also noted that the J_o and J_2 modes had a steady-state response that was second harmonic in time. These results were used as a guide in posing the steady state solution of boundary value problem [Equations (A.12) and (A.13)] in the form given in Equation (A.18).

where ψ_n and x_n satisfy Laplace's equation and only ψ_1 and x_1 depend upon time. The notation $\vec{r}$ means dependance upon r, θ, and z.

In this development, the arbitrary potential functions, ψ_n and x_n are chosen to identically satisfy Equation (A.14). The time varying generalized coordinate associated with each of the potential functions is selected to approximately satisfy free-surface condition Equation (A.15). The approximate satisfaction of Equation (A.15) is carried out by first introducing Equation (A.18) into (A.15) and then requiring that the coefficients of $\epsilon^{1/3}$, $\epsilon^{2/3}$, and ϵ vanish for all time in a Rayleigh-Ritz sense. In the following work, it is noted that the coefficient of $\epsilon^{1/3}$ contains sin ωt and cos ωt terms; that the coefficient of $\epsilon^{2/3}$ contains sin $2\omega t$, cos $2\omega t$ terms; and terms independent of ωt; and finally, that the coefficient of ϵ contains sin ωt and cos ωt terms and also higher harmonic terms. The approximation imposed is that these terms all vanish identically for the $\epsilon^{1/3}$ and $\epsilon^{2/3}$ terms and the first harmonic terms for ϵ.

When these steps are carried out, the transformations

$$\tau = \frac{1}{2}\epsilon^{2/3}\omega t \quad , \quad p_{11}^2 = \omega^2(1 - \nu\epsilon^{2/3}) \tag{A.19}$$

are introduced where the lowest natural frequency of small, free surface oscillations, p_{11}, is given by

$$p_{11} = \sqrt{g\lambda_{11} \tanh (\lambda_{11} h)} \tag{A.20}$$

and where λ_{11} corresponds to the first zero of $J_1'(\lambda_{11} a)$. Introducing (A.18) into (A.15), using (A.19), and then setting the coefficient of the $\epsilon^{1/3}$ terms equal to zero yields

$$\left(g\,\psi_{1z} - p_{11}^{\,2}\,\psi_1\right)\cos\omega t + \left(g x_{1z} - p_{11}^{\,2} x_1\right)\sin\omega t = 0 \quad \text{on} \quad z = 0 \ . \qquad \text{A.21)}$$

For these first-order terms to vanish for all time, it is necessary that

$$\psi_{1z} = \frac{p_{11}^{\,2}}{g}\,\psi_1 \quad \text{and} \quad x_{1z} = \frac{p_{11}^{\,2}}{g}\,x_1 \ . \qquad \text{(A.22)}$$

Equation (A.21) will be satisfied identically by choosing

$$\left.\begin{aligned} \psi_1 &= \left[f_1(\tau)\cos\theta + f_3(\tau)\sin\theta\right] J_1(\lambda_{11} r)\,\frac{\cosh\left[\lambda_{11}(z+h)\right]}{\cosh(\lambda_{11} h)} \ , \\ x_1 &= \left[f_2(\tau)\cos\theta + f_4(\tau)\sin\theta\right] J_1(\lambda_{11} r)\,\frac{\cosh\left[\lambda_{11}(z+h)\right]}{\cosh(\lambda_{11} h)} \ , \end{aligned}\right\} \qquad \text{(A.23)}$$

regardless of the values of the generalized coordinates f_i, providing

$$p_{11}^{\,2} = g\lambda_{11}\alpha_{11} \ , \quad \alpha_{11} \equiv \tanh(\lambda_{11} h) \ . \qquad \text{(A.24)}$$

For the second-order terms to vanish, the coefficient of $\epsilon^{2/3}$ must vanish. The resulting equation contains second harmonic terms in ωt and constant terms only. Setting the constant term and the $\cos(2\omega t)$ and $\sin(2\omega t)$ terms equal to zero and using the relations

$$x_1\psi_{1z} = x_{1z}\psi_1 \quad \text{and} \quad x_1\psi_{1zz} = x_{1zz}\psi_1 \ , \qquad \text{(A.25)}$$

obtained from Equations (A.22), reduces the three equations to

$$\psi_{0z} = 0 \ , \qquad \text{(A.26a)}$$

$$4p_{11}^2\psi_2 - g\psi_{2z} = 2p_{11}\left(x_{1r}\psi_{1r} + \frac{1}{r^2}x_{1\theta}\psi_{1\theta} + \frac{3a_{11}^2 - 1}{2}\lambda_{11}^2 x_1\psi_1\right), \tag{A.26b}$$

$$4p_{11}^2 x_2 - gx_{2z} = p_{11}\left[x_{1r}^2 - \psi_{1r}^2 + \frac{1}{r^2}x_{1\theta}^2 - \frac{1}{r^2}\psi_{1\theta}^2 + \frac{3a_{11}^2 - 1}{2}\lambda_{11}^2\left(x_1^2 - \psi_1^2\right)\right] . \tag{A.26c}$$

The arbitrary functions ψ_0, ψ_2, and x_2 are selected to satisfy Equations (A.26a, b, c). If ψ_0 is taken to be a constant, Equation (A.26a) will be satisfied identically. If ψ_2 and x_2 are taken to be

$$\psi_2 = \sum_{n=1}^{\infty} \hat{A}_{0n} J_0(\lambda_{0n} r) \frac{\cosh\left[\lambda_{0n}(z + h)\right]}{\cosh(\lambda_{0n} h)} + \sum_{n=1}^{\infty} (\hat{A}_{2n}\cos 2\theta + \hat{B}_{2n}\sin 2\theta) J_2(\lambda_{2n} r) \frac{\cosh\left[\lambda_{2n}(z + h)\right]}{\cosh(\lambda_{2n} h)} \tag{A.27a}$$

and

$$x_2 = \sum_{n=1}^{\infty} \hat{C}_{0n} J_0(\lambda_{0n} r) \frac{\cosh\left[\lambda_{0n}(z + h)\right]}{\cosh(\lambda_{0n} h)} + \sum_{n=1}^{\infty} (\hat{C}_{2n}\cos 2\theta + \hat{D}_{2n}\sin 2\theta) J_2(\lambda_{2n} r) \frac{\cosh\left[\lambda_{2n}(z + h)\right]}{\cosh(\lambda_{2n} h)} , \tag{A.27b}$$

where

$$J_0'(\lambda_{0n} a) = J_2'(\lambda_{2n} a) = 0 , \tag{A.28}$$

then Equations (A.26b) and (A.26c) can be satisfied by choosing the suitable generalized coordinates in ψ_2 and x_2. These generalized

coordinates can be expressed in terms of f_1, f_2, f_3, and f_4 by introducing Equations (A.23) and (A.27a, b) into (A.26b, c) and applying the Fourier-Bessel techniques in which the following orthogonality relations are used:

$$\int_o^a r J_0(\lambda_{0m} r) J_0(\lambda_{0n} r) dr = \begin{cases} 0 & , \quad m \neq n \\ \frac{a^2}{2} J_0^2(\lambda_{0n} a) & , \quad m = n \end{cases} \qquad \text{(A.29a)}$$

$$\int_o^a r J_2(\lambda_{2m} r) J_2(\lambda_{2n} r) dr = \begin{cases} 0 & , \quad m \neq n \\ \frac{\lambda_{2n}^2 a^2 - 4}{2\lambda_{2n}^2} J_2^2(\lambda_{2n} a) & , \quad m = n \end{cases} . \qquad \text{(A.29b)}$$

In this manner, the generalized coordinates of the J_0 and J_2 modes can be expressed in terms of the f_i. This process yields

$$\left.\begin{aligned} \hat{A}_{0n} &= \Omega_{0n}(f_1 f_2 + f_3 f_4) \quad , \quad \hat{C}_{0n} = \Omega_{0n} \tfrac{1}{2}\left(f_2^2 + f_4^2 - f_1^2 - f_3^2\right) , \\ \hat{A}_{2n} &= \Omega_{2n}(f_1 f_2 - f_3 f_4) \quad , \quad \hat{C}_{2n} = \Omega_{2n} \tfrac{1}{2}\left(f_2^2 + f_3^2 - f_1^2 - f_4^2\right) , \\ \hat{B}_{2n} &= \Omega_{2n}(f_1 f_4 + f_2 f_3) \quad , \quad \hat{D}_{2n} = \Omega_{2n}\left(f_2 f_4 - f_1 f_3\right) , \end{aligned}\right\} \qquad \text{(A.30)}$$

where

$$\left.\begin{aligned} \Omega_{0n} &= \frac{I_{01}^{\,n} + I_{02}^{\,n} + K_0 I_{03}^{\,n}}{\left(4p_{11}^{\,2} - p_{0n}^{\,2}\right)\frac{a^2}{2p_{11}} J_0^{\,2}(\lambda_{0n}a)} , \\ \Omega_{2n} &= \frac{I_{21}^{\,n} - I_{22}^{\,n} + K_0 I_{23}^{\,n}}{\left(4p_{11}^{\,2} - p_{2n}^{\,2}\right)\frac{\lambda_{2n}^{\,2}a^2 - 4}{2\lambda_{2n}^{\,2}p_{11}} J_2^{\,2}(\lambda_{2n}a)} , \end{aligned}\right\} \qquad (A.31)$$

and

$$\left.\begin{aligned} I_{q1}^{\,n} &= \int_0^{\lambda_{11}a} uJ_q\left(\frac{\lambda_{qn}}{\lambda_{11}}u\right)\left[\frac{d}{du}J_1(u)\right]^2 du \ , \quad q = 0,\ 2 \ , \\ I_{q2}^{\,n} &= \int_0^{\lambda_{11}a} \frac{1}{u} J_q\left(\frac{\lambda_{qn}}{\lambda_{11}}u\right) J_1^{\,2}(u)du \ , \quad q = 0,\ 2 \ , \\ I_{q3}^{\,n} &= \int_0^{\lambda_{11}a} uJ_q\left(\frac{\lambda_{qn}}{\lambda_{11}}u\right) J_1^{\,2}(u)du \ , \quad q = 0,\ 2 \ , \\ K_o &= \frac{3a_{11}^{\,2} - 1}{2} \ . \end{aligned}\right\} \qquad (A.32)$$

The coefficient of ϵ yields the third-order terms. Third-order terms arise from each of the boundary value terms, B_1, B_2, and B_3. For the third-order terms, it is only required that the first harmonic terms vanish. The first harmonic terms from B_1 are

$$p_{11}^2\left[\left(\frac{dx_1}{d\tau} - \nu\psi_1 - r\cos\theta\right)\cos\omega t - \left(\frac{d\psi_1}{d\tau} + \nu x_1\right)\sin\omega t\right] \qquad \text{(A.33a)}$$

and the first harmonic terms from B_2 are

$$p_{11}\Big[\psi_{1r}x_{2r} - x_{1r}\psi_{2r} + \frac{1}{r^2}(\psi_{1\theta}x_{2\theta} - x_{1\theta}\psi_{2\theta}) - \lambda_{11}^2\left(a_{11}^2 - 1\right)(x_1\psi_2 - \psi_1 x_2)$$
$$- \lambda_{11}a_{11}(\psi_1 x_{2z} - x_1\psi_{2z}) + \frac{1}{2}(\psi_1 x_{2zz} - x_1\psi_{2zz})\Big]\cos\omega t - p_{11}\Big[x_{1r}x_{2r} + \psi_{1r}\psi_{2r}$$
$$+ \frac{1}{r^2}(x_{1\theta}x_{2\theta} + \psi_{1\theta}\psi_{2\theta}) + \lambda_{11}^2\left(a_{11}^2 - 1\right)(x_1x_2 + \psi_1\psi_2) - \lambda_{11}a_{11}(x_1x_{2z}$$
$$+ \psi_1\psi_{2z} + \frac{1}{2}(x_1x_{2zz} + \psi_1\psi_{2zz})\Big]\sin\omega t \ . \qquad \text{(A.33b)}$$

Similarly, there are first harmonic terms from B_3 which are lengthly expressions and are not presented because it is the integrals of B_1, B_2, and B_3 that are required in the Rayleigh-Ritz procedure. Introducing Equations (A.23) into the expressions for B_1, B_2, and B_3 and using Equations (A.30) to evaluate the contribution from B_2 results in the following integrals:

$$\int_0^a\int_0^{2\pi} B_1\cos\theta\, J_1(\lambda_{11}r)\,r\,dr\,d\theta$$

$$= \pi p_{11}^2\left[\frac{\lambda_{11}^2a^2 - 1}{2\lambda_{11}^2}J_1^2(\lambda_{11}a)\left(\frac{df_2}{d\tau} - \nu f_1\right)\right.$$

$$\left. - \frac{a}{\lambda_{11}^2}J_1(\lambda_{11}a)\right]\cos\omega t$$

$$- \pi p_{11}^2\left[\frac{\lambda_{11}^2a^2 - 1}{2\lambda_{11}^2}J_1^2(\lambda_{11}a)\left(\frac{df_1}{d\tau} + \nu f_2\right)\right]\sin\omega t \ , \qquad \text{(A.34a)}$$

$$\int_o^a \int_o^{2\pi} B_1 \sin\theta\, J_1(\lambda_{11} r) r\, dr\, d\theta$$

$$= \pi p_{11}^2 \left[\frac{\lambda_{11}^2 a^2 - 1}{2\lambda_{11}^2} J_1^2(\lambda_{11} a) \left(\frac{df_4}{d\tau} - \nu f_3 \right) \right] \cos \omega t \qquad \text{(A.34b)}$$

$$- \pi p_{11}^2 \left[\frac{\lambda_{11}^2 a^2 - 1}{2\lambda_{11}^2} J_1^2(\lambda_{11} a) \left(\frac{df_3}{d\tau} + \nu f_4 \right) \right] \sin \omega t \ ,$$

$$\int_o^a \int_o^{2\pi} B_2 \cos\theta\, J_1(\lambda_{11} r) r\, dr\, d\theta$$

$$= \pi p_{11} \Big[f_1 \left(f_1^2 + f_2^2 + f_3^2 + f_4^2 \right) \hat{G}_1$$

$$+ f_4 (f_2 f_3 - f_1 f_4) \hat{G}_2 \Big] \cos \omega t$$

$$+ \pi p_{11} \Big[f_2 \left(f_1^2 + f_2^2 + f_3^2 + f_4^2 \right) \hat{G}_1$$

$$- f_3 (f_2 f_3 - f_1 f_4) \hat{G}_2 \Big] \sin \omega t \ , \qquad \text{(A.34c)}$$

$$\int_o^a \int_o^{2\pi} B_2 \sin\theta\, J_1(\lambda_{11} r) r\, dr\, d\theta$$

$$= \pi p_{11} \Big[f_3 \left(f_1^2 + f_2^2 + f_3^2 + f_4^2 \right) \hat{G}_1$$

$$- f_2 (f_2 f_3 - f_1 f_4) \hat{G}_2 \Big] \cos \omega t$$

$$+ \pi p_{11} \Big[f_4 \left(f_1^2 + f_2^2 + f_3^2 + f_4^2 \right) \hat{G}_1$$

$$+ f_1 (f_2 f_3 - f_1 f_4) \hat{G}_2 \Big] \sin \omega t \ , \qquad \text{(A.34d)}$$

$$\int_o^a \int_o^{2\pi} B_3 \cos\theta\, J_1(\lambda_{11} r) r\, dr\, d\theta$$

$$= -\frac{1}{4} p_{11}{}^2 \left[f_1 \left(f_1{}^2 + f_2{}^2 + f_3{}^2 + f_4{}^2 \right) \hat{H}_1 + f_4 (f_2 f_3 - f_1 f_4) \hat{H}_2 \right] \cos \omega t - \frac{1}{4} p_{11}{}^2 \left[f_2 \left(f_1{}^2 + f_2{}^2 + f_3{}^2 + f_4{}^2 \right) \hat{H}_1 - f_3 (f_2 f_3 - f_1 f_4) \hat{H}_2 \right] \sin \omega t \quad , \tag{A.34e}$$

$$\int_o^a \int_o^{2\pi} B_3 \sin\theta\, J_1(\lambda_{11} r) r\, dr\, d\theta$$

$$= -\frac{1}{4} p_{11}{}^2 \left[f_3 \left(f_1{}^2 + f_2{}^2 + f_3{}^2 + f_4{}^2 \right) \hat{H}_1 - f_2 (f_2 f_3 - f_1 f_4) \hat{H}_2 \right] \cos \omega t - \frac{1}{4} p_{11}{}^2 \left[f_4 \left(f_1{}^2 + f_2{}^2 + f_3{}^2 + f_4{}^2 \right) \hat{H}_1 + f_1 (f_2 f_3 - f_1 f_4) \hat{H}_2 \right] \sin \omega t \quad , \tag{A.34f}$$

where

$$\hat{G}_1 = \frac{1}{2} \sum_{n=1}^{\infty} \left\{ \left[\alpha_{0n} \alpha_{11} \lambda_{0n} \lambda_{11} - \frac{1}{2} \lambda_{0n}{}^2 + \lambda_{11}{}^2 \left(1 - \alpha_{11}{}^2 \right) \right] \Omega_{0n} I_{03}{}^n - \Omega_{0n} I_{04}{}^n - \Omega_{2n} I_{22}{}^n - \frac{1}{2} \Omega_{2n} I_{24}{}^n + \frac{1}{2} \left[\alpha_{11} \alpha_{2n} \lambda_{11} \lambda_{2n} - \frac{1}{2} \lambda_{2n}{}^2 + \lambda_{11}{}^2 \left(1 - \alpha_{11}{}^2 \right) \right] \Omega_{2n} I_{23}{}^n \right\} \quad , \tag{A-35a}$$

$$\hat{G}_2 = \sum_{n=1}^{\infty}\left\{\left[a_{0n}a_{11}\lambda_{0n}\lambda_{11} - \frac{1}{2}\lambda_{0n}^{\,2} + \lambda_{11}^{\,2}\left(1 - a_{11}^{\,2}\right)\right]\Omega_{0n}I_{03}^{\,n} - \Omega_{0n}I_{04}^{\,n} + \Omega_{2n}I_{22}^{\,n} + \frac{1}{2}\Omega_{2n}I_{24}^{\,n} - \frac{1}{2}\left[a_{11}a_{2n}\lambda_{11}\lambda_{2n} - \frac{1}{2}\lambda_{2n}^{\,2} + \lambda_{11}^{\,2}\left(1 - a_{11}^{\,2}\right)\right]\Omega_{2n}I_{23}^{\,n}\right\} , \qquad \text{(A.35b)}$$

$$\left.\begin{aligned}
\hat{H}_1 &= 3k_1 + k_2 , & k_1 &= \frac{\pi}{2}\frac{\lambda_{11}^{\,2}}{Kp_{11}^{\,2}}k_{10} ,\\
\hat{H}_2 &= 2(k_1 - k_3 + k_4) , & k_2 &= \frac{\pi}{2}\frac{\lambda_{11}}{Kga_{11}}k_{20} ,\\
a_{mn} &= \tanh(\lambda_{mn}h) , & k_3 &= \frac{\pi}{2}\frac{\lambda_{11}}{Kga_{11}}k_{30} ,\\
p_{mn}^{\,2} &= g\lambda_{mn}a_{mn} , & k_4 &= \frac{\pi}{2}\frac{\lambda_{11}}{Kga_{11}}k_{40} ,\\
k_{10} &= -\frac{1}{4}K\left[6I_1 - I_3 - 2I_4 - 3I_5 + 4I_6 - 2I_7 + a_{11}^{\,2}(3I_2 + 5I_3 + 15I_5) + 3a_{11}^{\,4}I_2\right] ,\\
k_{20} &= \frac{1}{2}Ka_{11}^{\,2}\left(9I_2 + 4I_3 + 12I_5 + 3a_{11}^{\,2}I_2\right) ,\\
k_{30} &= \frac{1}{2}Ka_{11}^{\,2}\left(3I_2 - 4I_3 + 4I_5 + a_{11}^{\,2}I_2\right) ,\\
k_{40} &= Ka_{11}^{\,2}\left(3I_2 + 4I_3 + 4I_5 + a_{11}^{\,2}I_2\right) ,
\end{aligned}\right\} \qquad \text{(A.36)}$$

$$
\left.
\begin{aligned}
K &= \frac{1}{\left(\lambda_{11}^2 a^2 - 1\right) J_1^2(\lambda_{11} a)} \left(\frac{\lambda_{11}^3}{g a_{11}}\right), \\
I_1 &= \int_0^{\lambda_{11} a} u J_1 \left(\frac{dJ_1}{du}\right)^2 \frac{d^2 J_1}{du^2}\, du = \frac{1}{\lambda_{11}^2} \int_0^a r J_1 \left(\frac{dJ_1}{dr}\right)^2 \frac{d^2 J_1}{dr^2}\, dr \\
I_2 &= \int_0^{\lambda_{11} a} u J_1^4 du = \lambda_{11}^2 \int_0^a r J_1^4 dr , \\
I_3 &= \int_0^{\lambda_{11} a} \frac{1}{u} J_1^4 du = \int_0^a \frac{1}{r} J_1^4 dr , \\
I_4 &= \int_0^{\lambda_{11} a} \frac{1}{u^3} J_1^4 du = \frac{1}{\lambda_{11}^2} \int_0^a \frac{1}{r^3} J_1^4 dr , \\
I_5 &= \int_0^{\lambda_{11} a} u J_1^2 \left(\frac{dJ_1}{du}\right)^2 du = \int_0^a r J_1^2 \left(\frac{dJ_1}{dr}\right)^2 dr , \\
I_6 &= \int_0^{\lambda_{11} a} \frac{1}{u} J_1^2 \left(\frac{dJ_1}{du}\right)^2 du = \frac{1}{\lambda_{11}^2} \int_0^a \frac{1}{r} J_1^2 \left(\frac{dJ_1}{dr}\right)^2 dr , \\
I_7 &= \int_0^{\lambda_{11} a} \frac{1}{u^2} J_1^3 \left(\frac{dJ_1}{du}\right) du = \frac{1}{\lambda_{11}^2} \int_0^a \frac{1}{r^2} J_1^3 \left(\frac{dJ_1}{dr}\right) dr . \\
I_{q4}^n &= \int_0^{\lambda_{11} a} u J_1(u) \frac{d}{du} \left[J_1(u)\right] \frac{d}{du} \left[J_q\left(\frac{\lambda_{qn}}{\lambda_{11}} u\right)\right] du , \quad q = 0, 2 .
\end{aligned}
\right\} \text{(A.36) (Cont.)}
$$

Two ordinary differential equations are obtained by introducing the potential function Equations (A.18) into (A.15) and then carrying out the Rayleigh-Ritz procedure by first multiplying by $J_1(\lambda_{11}r)$ cos θ rdr dθ and integrating over $0 \leq r \leq a$ and $0 \leq \theta \leq 2\pi$, then multiplying by $J_1(\lambda_{11}r)$ sin θr dr dθ and integrating throughout the same region. Then, the first harmonic terms in ω are set equal to zero in both of these equations, producing the following four first-order nonlinear differential equations:

$$\left.\begin{aligned}
\frac{df_1}{d\tau} &= -\nu f_2 - K_1 f_2\left(f_1^2 + f_2^2 + f_3^2 + f_4^2\right) + K_2 f_3(f_2 f_3 - f_1 f_4) \ , \\
\frac{df_2}{d\tau} &= F_1 + \nu f_1 + K_1 f_1\left(f_1^2 + f_2^2 + f_3^2 + f_4^2\right) + K_2 f_4(f_2 f_3 - f_1 f_4) \ , \\
\frac{df_3}{d\tau} &= -\nu f_4 - K_1 f_4\left(f_1^2 + f_2^2 + f_3^2 + f_4^2\right) - K_2 f_1(f_2 f_3 - f_1 f_4) \ , \\
\frac{df_4}{d\tau} &= \nu f_3 + K_1 f_3\left(f_1^2 + f_2^2 + f_3^2 + f_4^2\right) - K_2 f_2(f_2 f_3 - f_1 f_4) \ .
\end{aligned}\right\} \qquad \text{(A.37)}$$

where

$$\left.\begin{aligned}
K_1 &= K_{10} + \Delta K_1 \\
K_2 &= K_{20} + \Delta K_2 \\
F_1 &= \frac{2a}{\left(\lambda_{11}^2 a^2 - 1\right) J_1(\lambda_{11} a)}
\end{aligned}\right\} \qquad \text{(A.38a)}$$

and

$$
\left.
\begin{aligned}
K_{10} &= \frac{1}{16} K\Big[-18I_1 + 3I_3 + 6I_4 + 9I_5 - 12I_6 + 6I_7 \\
&\quad + a_{11}^2(9I_2 - 7I_3 - 21I_5) - 3a_{11}^4 I_2\Big] , \\
K_{20} &= \frac{1}{8} K\Big[-6I_1 + I_3 + 2I_4 + 3I_5 - 4I_6 + 2I_7 \\
&\quad + a_{11}^2(3I_2 + 19I_3 - 7I_5) - a_{11}^4 I_2\Big] , \\
\Delta K_1 &= -\frac{2p_{11}}{\lambda_{11}^2} K\hat{G}_1 , \\
\Delta K_2 &= -\frac{2p_{11}}{\lambda_{11}^2} K\hat{G}_2 .
\end{aligned}
\right\} \quad \text{(A.38b)}
$$

The form of Equations (A.37) is identical with that of the set of differential equations derived by Miles[5] for the undamped spherical pendulum. Therefore, the steady-state solutions of Equations (A.37) are the same as the two obtained by Miles for the spherical pendulum.

These two steady-state harmonic solutions correspond to the zeros of $df_i/d\tau$ for i = 1, 2, 3, 4. The first solution, called planar motion, is a steady-state fluid motion with a constant peak wave height and a single, stationary nodal dimeter perpendicular to the direction of excitation. The second solution, called nonplanar motion, is a steady-state fluid motion with a constant peak wave height and a single nodal diameter that rotates at a constant rate around the container. For the planar motion, the solution is

$$f_1 = \gamma , \quad f_2 = f_3 = f_4 = 0 , \qquad \text{(A.39a)}$$

with

$$\nu = - F_1 \gamma^{-1} - K_1 \gamma^2 \quad . \tag{A.39b}$$

For the nonplanar motion, the solution is

$$f_1 = \gamma \ , \quad f_2 = f_3 = 0 \ , \quad f_4^2 = \zeta^2 = \gamma^2 + \frac{F_1}{K_2} \gamma^{-1} \ , \tag{A.40a}$$

with

$$\nu = - K_3 \gamma^{-1} + K_4 \gamma^2 \quad , \tag{A.40b}$$

where

$$K_3 = \frac{K_1}{K_2} F_1 \ , \quad K_4 = K_2 - 2K_1 \quad . \tag{A.41}$$

This solution is real, and hence exists, for $\lambda > 0$ when $\gamma^3 + F_1/K_2 > 0$ and for $\gamma < 0$ when $\gamma^3 + F_1/K_2 < 0$.

4. Stability of Steady-State Harmonic Solutions

Stability of the steady-state harmonic solutions obtained in the preceding section will now be investigated. A particular steady-state harmonic solution of Equations (A. 37) is denoted by the superscript (o), and the stability of such solutions is investigated by imposing a small perturbation from this steady-state solution and examining the subsequent motion. If the motion following the perturbation decreases with time, the solution is called stable; if the motion increases with time, the solution is called unstable. Mathematically, set

$$f_i(\tau) = f_i^{(o)} + c_i \, e^{\lambda \tau} \quad , \tag{A.42}$$

where $f_i^{(o)}$ are constants corresponding to the steady-state amplitudes of the harmonic solutions of Equations (A.37) and the c_i are assumed to be small. Stable $f_i^{(o)}$ solutions correspond to values of λ with negative real part, and unstable solutions correspond to correspond to values of λ with positive real part. Introducing Equation (A.42) into Equations (A.37) neglecting products of c_1, and imposing the condition that the $f_i^{(o)}$ are solutions of Equations (A.37) leads to the following set of homogeneous algebraic equations:

$$\begin{bmatrix} d_{11}+\lambda & d_{12} & d_{13} & d_{14} \\ d_{21} & d_{22}-\lambda & d_{23} & d_{24} \\ d_{31} & d_{32} & d_{33}+\lambda & d_{34} \\ d_{41} & d_{42} & d_{43} & d_{44}-\lambda \end{bmatrix} \begin{Bmatrix} c_1 \\ c_2 \\ c_3 \\ c_4 \end{Bmatrix} = \begin{Bmatrix} 0 \\ 0 \\ 0 \\ 0 \end{Bmatrix} \quad \text{(A.43)}$$

where

$$
\left.
\begin{aligned}
d_{11} &= 2K_1 f_1^{(o)} f_2^{(o)} + K_2 f_3^{(o)} f_4^{(o)} \quad , \\
d_{12} &= \nu + K_1\left[f_1^{(o)2} + 3f_2^{(o)2} + f_3^{(o)2} + f_4^{(o)2}\right] - K_2 f_3^{(o)2} \quad , \\
d_{13} &= 2K_1 f_2^{(o)} f_3^{(o)} + K_2\left[f_1^{(o)} f_4^{(o)} - 2f_2^{(o)} f_3^{(o)}\right] \quad , \\
d_{14} &= 2K_1 f_2^{(o)} f_4^{(o)} + K_2 f_1^{(o)} f_3^{(o)} \quad , \\
d_{21} &= \nu + K_1\left[3f_1^{(o)2} + f_2^{(o)2} + f_3^{(o)2} + f_4^{(o)2}\right] - K_2 f_4^{(o)2} \quad , \\
d_{22} &= d_{11} \quad , \\
d_{23} &= 2K_1 f_1^{(o)} f_3^{(o)} + K_2 f_2^{(o)} f_4^{(o)} \quad , \\
d_{24} &= 2K_1 f_1^{(o)} f_4^{(o)} + K_2\left[f_2^{(o)} f_3^{(o)} - 2f_1^{(o)} f_4^{(o)}\right] \quad ,
\end{aligned}
\right\} \quad (A.44)
$$

$$
\left.
\begin{aligned}
d_{31} &= d_{24} \ , \\
d_{32} &= d_{14} \ , \\
d_{33} &= 2K_1 f_3^{(o)} f_4^{(o)} + K_2 f_1^{(o)} f_2^{(o)} \ , \\
d_{34} &= \nu + K_1\left[f_1^{(o)2} + f_2^{(o)2} + f_3^{(o)2} + 3f_4^{(o)2}\right] - K_2 f_1^{(o)2} \ , \\
d_{41} &= d_{23} \ , \\
d_{42} &= d_{13} \ , \\
d_{43} &= \nu + K_1\left[f_1^{(o)2} + f_2^{(o)2} + 3f_3^{(o)2} + f_4^{(o)2}\right] - K_2 f_2^{(o)2} \ , \\
d_{44} &= d_{33} \ .
\end{aligned}
\right\} \quad \text{(A.44) (Cont.)}
$$

Since Equation (A.43) is a homogeneous set of equations in c_i, nontrivial solutions will exist only if the determinant of the coefficients in zero. Setting this determinant equal to zero yields the allowable values of λ. The question of stability reduces to an examination of the roots of the resulting equation in λ.

a. Planar Motion Solution

The steady-state planar motion solution found in this section was given as

$$f_1^{(o)} = \lambda \quad , \quad f_2^{(o)} = f_3^{(o)} = f_4^{(o)} = 0 \quad , \tag{A.45a}$$

where

$$\nu = -F_1\gamma^{-1} - K_1\gamma^2 \quad . \tag{A.45b}$$

Introducing Equations (A.45a) into Equation (A.43), setting the determinant of the coefficients of c_i equal to zero, and expanding results in

$$\lambda^4 + (M_1 + M_2)\lambda^2 + M_1 M_2 = 0 \quad , \tag{A.46}$$

where

$$\left.\begin{aligned} M_1 &= \begin{vmatrix} \nu + K_1\gamma^2 & 0 \\ 0 & \nu + 3K_1\gamma^2 \end{vmatrix} \\ M_2 &= \begin{vmatrix} \nu + K_1\gamma^2 & 0 \\ 0 & \nu + (K_1 - K_2)\gamma^2 \end{vmatrix} \end{aligned}\right\} \tag{A.47}$$

The roots of Equation (A.46) are

$$\lambda_1^2 = -M_1 = -\left(\nu + K_1\gamma^2\right)\left(\nu + 3K_1\gamma^2\right) = -F_1\gamma^{-1}\left(F_1\gamma^{-1} - 2K_1\gamma^2\right) \quad \text{(A.48a)}$$

and

$$\lambda_2^2 = -M_2 = -\left(\nu + K_1\gamma^2\right)\left[\nu + (K_1 - K_2)\gamma^2\right] = -F_1\gamma^{-1}\left(F_1\gamma^{-1} + K_2\gamma^2\right) . \quad \text{(A.48b)}$$

The boundary between stable and unstable planar motion corresponds to $\lambda_1 = 0$ and $\lambda_2 = 0$. From $\lambda_1^2 = 0$, it is found that:

$$\gamma = \pm\infty \quad \text{and} \quad \gamma = \left(\frac{F_1}{2K_1}\right)^{1/3} . \quad \text{(A.49a)}$$

Later, it is seen that $K_1 > 0$, so that from Equation (A.45b) these values correspond to

$$\nu = -\infty \quad \text{and} \quad \nu = -3K_1\left(\frac{F_1}{2K_1}\right)^{2/3} . \quad \text{(A.49b)}$$

From $\lambda_2^2 = 0$,

$$\gamma = \pm\infty \quad \text{and} \quad \gamma = -\left(\frac{F_1}{K_2}\right)^{1/3} \quad \text{(A.50a)}$$

are obtained.

When Equation (A.45b) is used with $K_1 > 0$, it is found that these values correspond to

$$\nu = -\infty \quad \text{and} \quad \nu = (K_2 - K_1)\left(\frac{F_1}{K_2}\right)^{2/3} . \quad \text{(A.50b)}$$

Figure 2 summarizes the regions of stable and unstable planar motion.

b. Nonplanar Motion Solution

The steady-state nonplanar motion found in this section was given as

$$f_1^{(o)} = \gamma, \quad f_2^{(o)} = f_3^{(o)} = 0 , \quad f_4^{(o)^2} = \zeta^2 = \gamma^2 + \frac{F_1}{K_2}\gamma^{-1} , \quad \text{(A.51a)}$$

where

$$\nu = - K_3\gamma^{-1} + K_4\gamma^2 \quad \text{(A.51b)}$$

The requirement that ζ be real demands that $\zeta^2 > 0$, which, in turn, indicates that this solution is not valid when γ lies in the range

$$- \frac{F_1}{K_2} < \gamma^3 < 0 \quad . \quad \text{(A.52)}$$

Introducing Equations (A.51a) into Equation (A.43), setting the determinant of the coefficients of c_i equal to zero, and expanding results in

$$\lambda^4 + (M_3 + M_4)\lambda^2 + M_5M_6 = 0 , \quad \text{(A.53)}$$

where

$$\left.\begin{aligned} M_3 &= \begin{vmatrix} d_{34} & d_{13} \\ d_{24} & d_{12} \end{vmatrix}, \quad M_4 = \begin{vmatrix} d_{12} & d_{13} \\ d_{24} & d_{21} \end{vmatrix} \\ M_5 &= \begin{vmatrix} d_{13} & d_{12} \\ d_{12} & d_{13} \end{vmatrix}, \quad M_6 = \begin{vmatrix} d_{24} & d_{21} \\ d_{34} & d_{24} \end{vmatrix} \end{aligned}\right\} \tag{A.54}$$

and

$$\left.\begin{aligned} d_{12} &= \nu + K_1(\gamma^2 + \zeta^2) , \\ d_{13} &= K_2 \gamma \zeta , \\ d_{21} &= \nu + 3K_1\gamma^2 + (K_1 - K_2)\zeta^2 , \\ d_{24} &= 2(K_1 - K_2)\gamma\zeta , \\ d_{34} &= \nu + 3K_1\zeta^2 + (K_1 - K_2)\gamma^2 . \end{aligned}\right\} \tag{A.55}$$

Introducing Equation (A.51b) into Equations (A.55) and expanding Equations (A.54) yields

$$\left.\begin{aligned} M_3 + M_4 &= 4K_2^2 \gamma\left(\gamma^3 + \frac{3K_2 - 2K_1}{4K_2^2} F_1\right) , \\ M_5 M_6 &= 4K_2^2(K_2 - 2K_1)F_1\gamma^{-1}\left(\gamma^3 + \frac{F_1}{K_2}\right)\left[\gamma^3 + \frac{K_1 F_1}{2K_2(K_2 - 2K_1)}\right] . \end{aligned}\right\} \tag{A.56}$$

REFERENCES

1. Eulitz, W.R. and Glaser, R.F., "Comparative Experimental and Theoretical Considerations on the Mechanisms of Fluid Oscillations in Cylindrical Containers." Report MTP-M-S and M-61, Army Ballistic Missile Agency, Huntsville, Ala., 29 May 1961.

2. Berlot, R.R., "Production of Rotation in a Confined Liquid Through Translation Motion of the Boundaries," J.Appl. Mech., 26:513-516, Dec. 1959.

3. Milne-Thomson, T.M. Theoretical Hydrodynamics, 3rd ed., Macmillan, London, 1950.

4. British Association for the Advancement of Science, Bessel Functions, University Press, Cambridge, Eng., 1950-58, 2 vols. (Its Mathematical Tables, vol. 6 and 10) Part I, Functions of Orders Zero and Unity; Part II, Functions of Positive Integer Order.

5. Miles, J.W., "Stability of Forced Oscillations of A Spherical Pendulum," Quart. Appl. Math, 20:21-32, April 1962.

Table 1. Bessel Function Parameters

n	$\lambda_{0n}a$	$\lambda_{2n}a$	$J_0(\lambda_{0n}a)$	$J_2(\lambda_{2n}a)$
1	0	3.05	1	0.486496
2	3.832	6.71	-0.402759	-0.313528
3	7.016	9.97	0.300116	0.254744
4	10.150	13.2	-0.249636	-0.220787
5	13.324	16.3	0.218359	0.197717

Table 2. Computed Values of Parameters

n	I_n	I_{01}^n	I_{02}^n	I_{03}^n	I_{04}^n	I_{21}^n	I_{22}^n
1	-0.012954	0.123802	0.280783	4.20814	0	0.0246726	0.0850317
2	0.112804	0.0492073	0.0286232	-0.695032	-0.144672	0.0376257	0.0436175
3	0.060038	-0.000376789	-0.00454246	0.00828100	0.00571932	0.0170224	0.0150985
4	0.049677	0.0000340190	0.00192154	0.00577141	-0.00137331	0.00975184	0.0104800
5	0.017589	-0.0000170201	-0.000853933	0.000394171	0.000909018	0.00638522	0.00565661
6	0.025648						
7	0.033292						
8	0.404591						
9	1.07133						

n	I_{23}^n	I_{24}^n	Ω_{0n}	Ω_{2n}	K_{n0}	K_n
1	1.67044	0.0509058	0.00104050	0.00159638	0.39483×10^{-5}	0.485278×10^{-5}
2	0.00884779	-0.0804156	0.000212563	-0.00091975	1.77883×10^{-5}	1.37066×10^{-5}
3	-0.00116172	-0.0322478	-0.00150727	-0.000104001		3.02353
4	-0.00567662	-0.0207806	-0.000133973	0.0000427096		0.400104×10^{-5}
5	-0.00721478	-0.0127190	0.0000276341	-0.00000141327		

Note: $K_o = 0.97624$, $K = 0.96209 \times 10^{-4}$.

Table 3. Domain of Stable and Unstable Nonplanar Harmonic Motions

$-\infty < \nu < -0.03027$ $0 < \gamma < 64.47$ $117.6 < \lvert\zeta\rvert < \infty$	unstable, since Re(λ) is positive
$-0.03027 < \nu < \infty$ $64.47 < \gamma < \infty$ $117.6 < \lvert\zeta\rvert < \infty$	stable, since Re(λ) is negative
$0.06459 < \nu < \infty$ $-\infty < \gamma < -85.41$ $0 < \lvert\zeta\rvert < \infty$	unstable, since Re(λ) is positive
$\infty < \nu < 0.06459$ $-85.41 < \gamma < 0$	solution does not exist, since $\zeta^2 < 0$

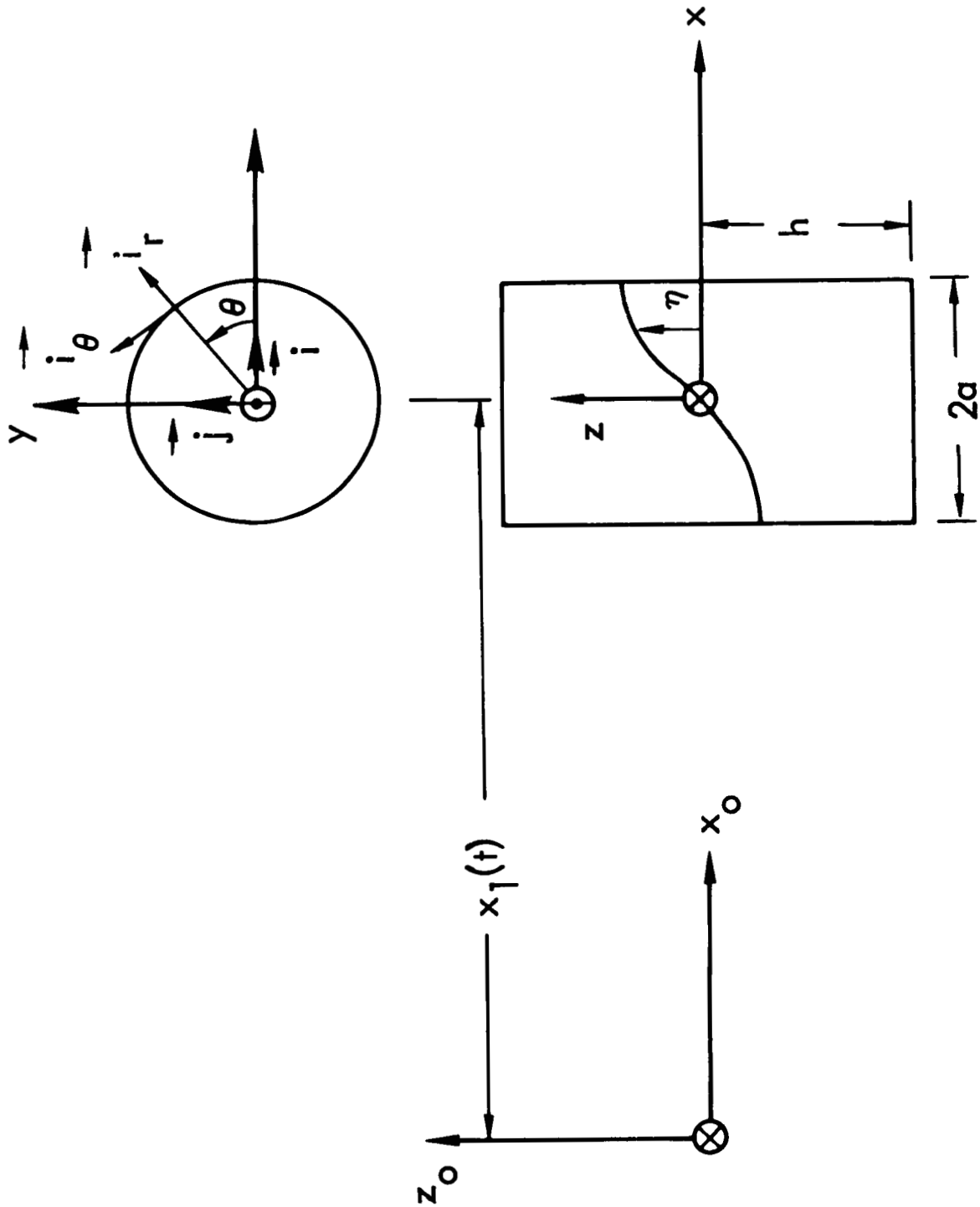

Figure 1. Coordinate Systems

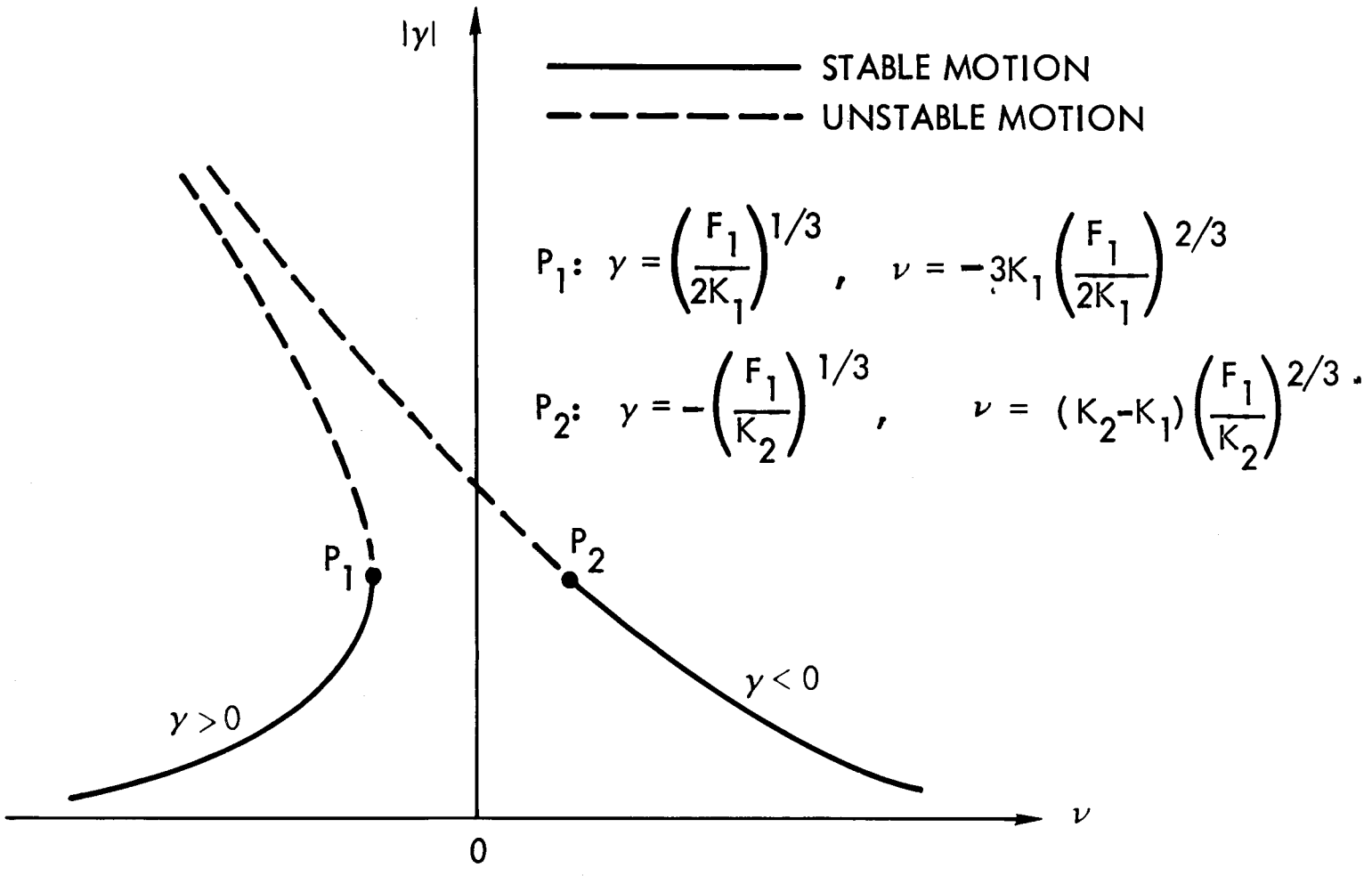

Figure 2. Planar Motion Amplitude/Frequency Relation

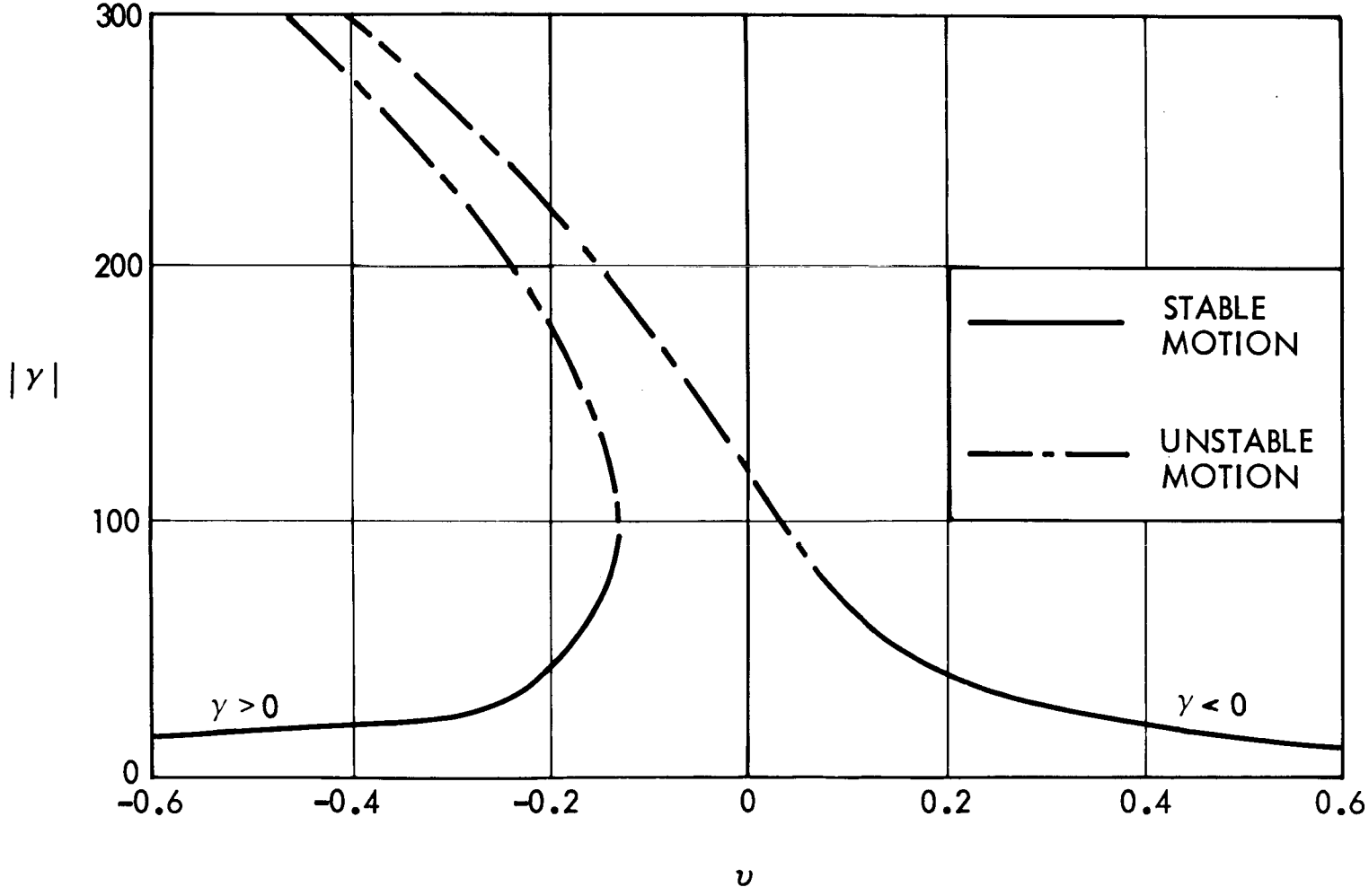

Figure 3. Planar Motion Amplitude/Frequency Relation, γ - ν

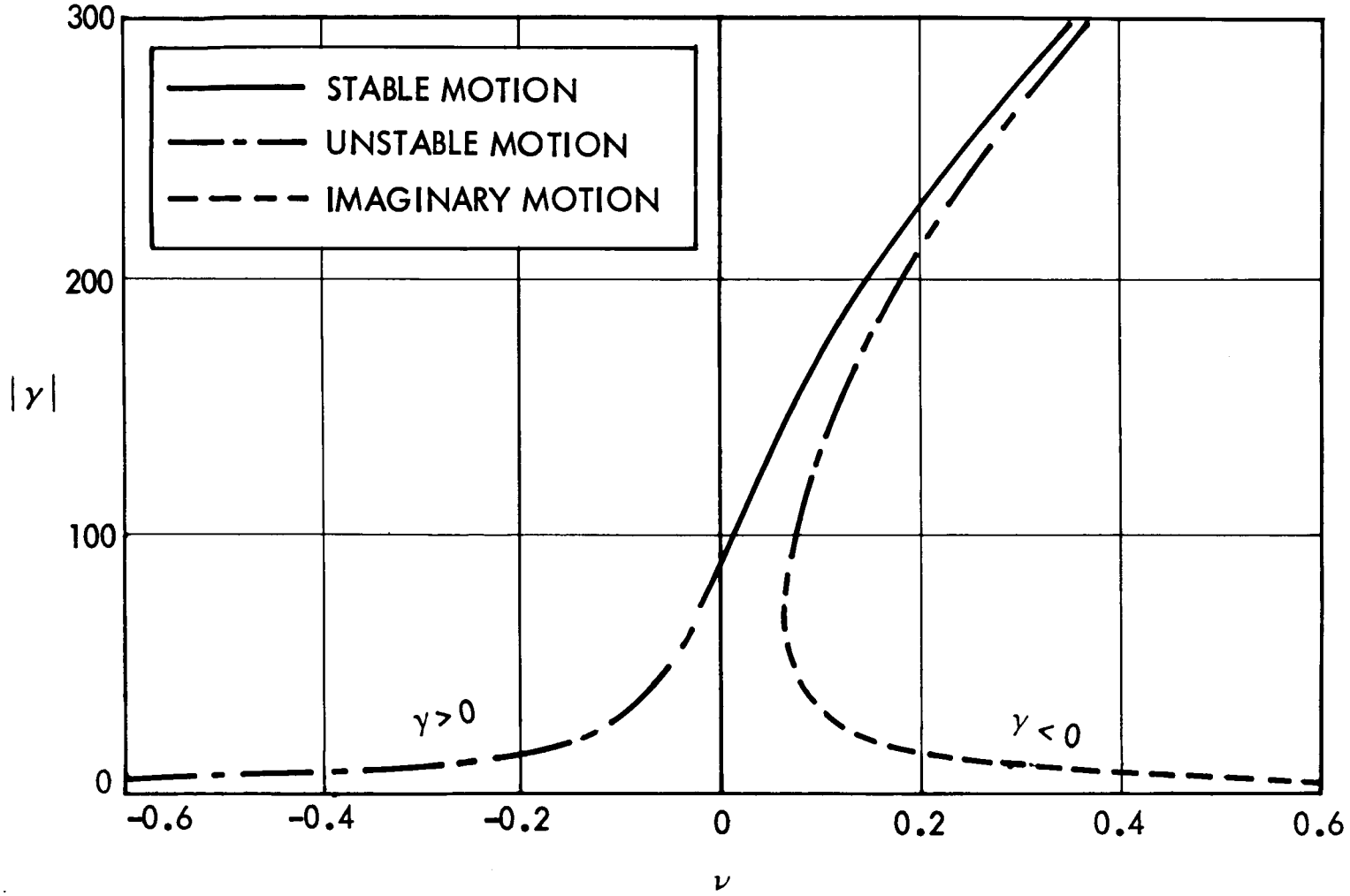

Figure 4. Nonplanar Motion Amplitude/Frequency Relation, γ - ν

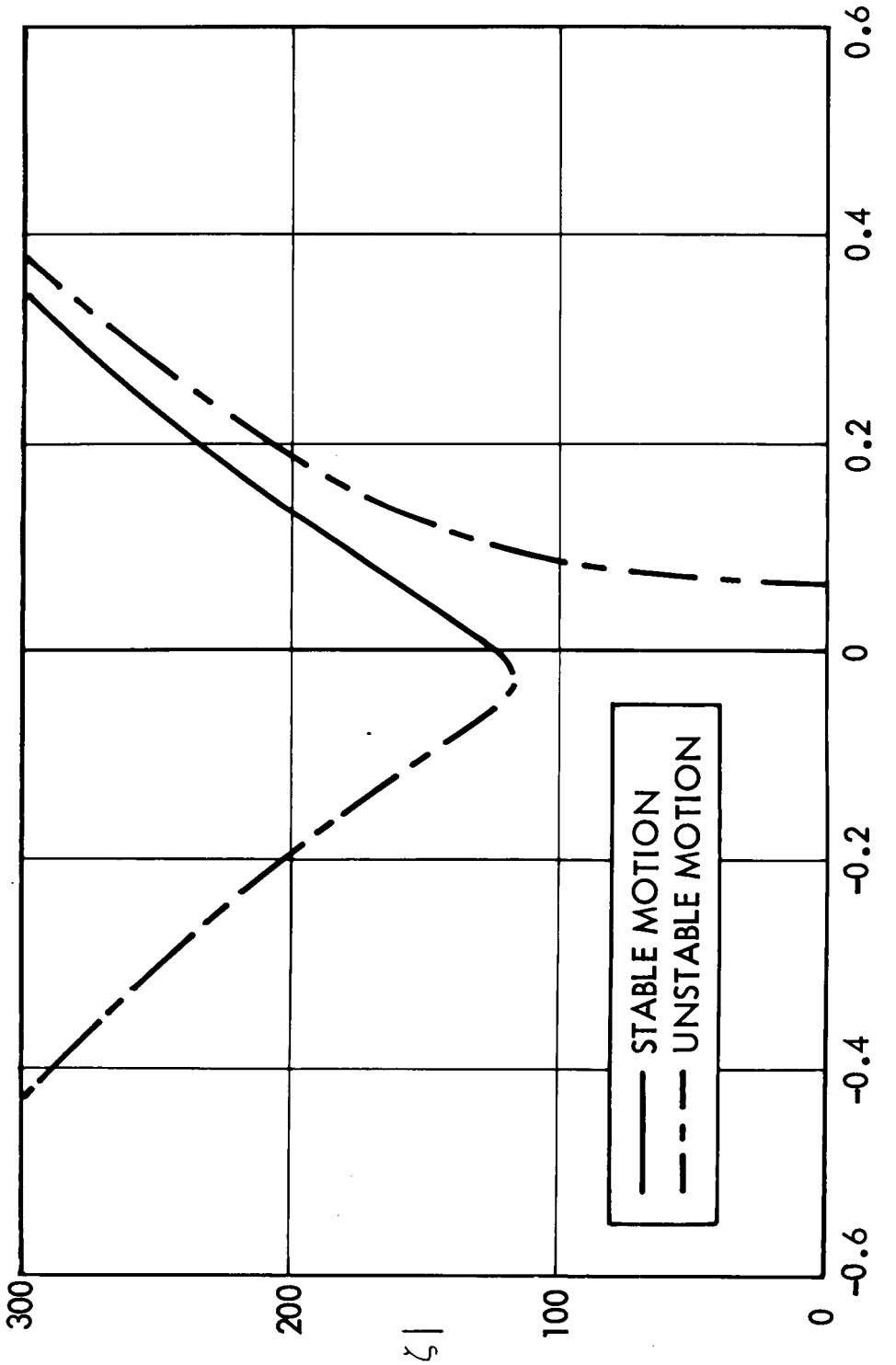

Figure 5. Nonplanar Motion Amplitude/Frequency Relation, $\zeta - \nu$

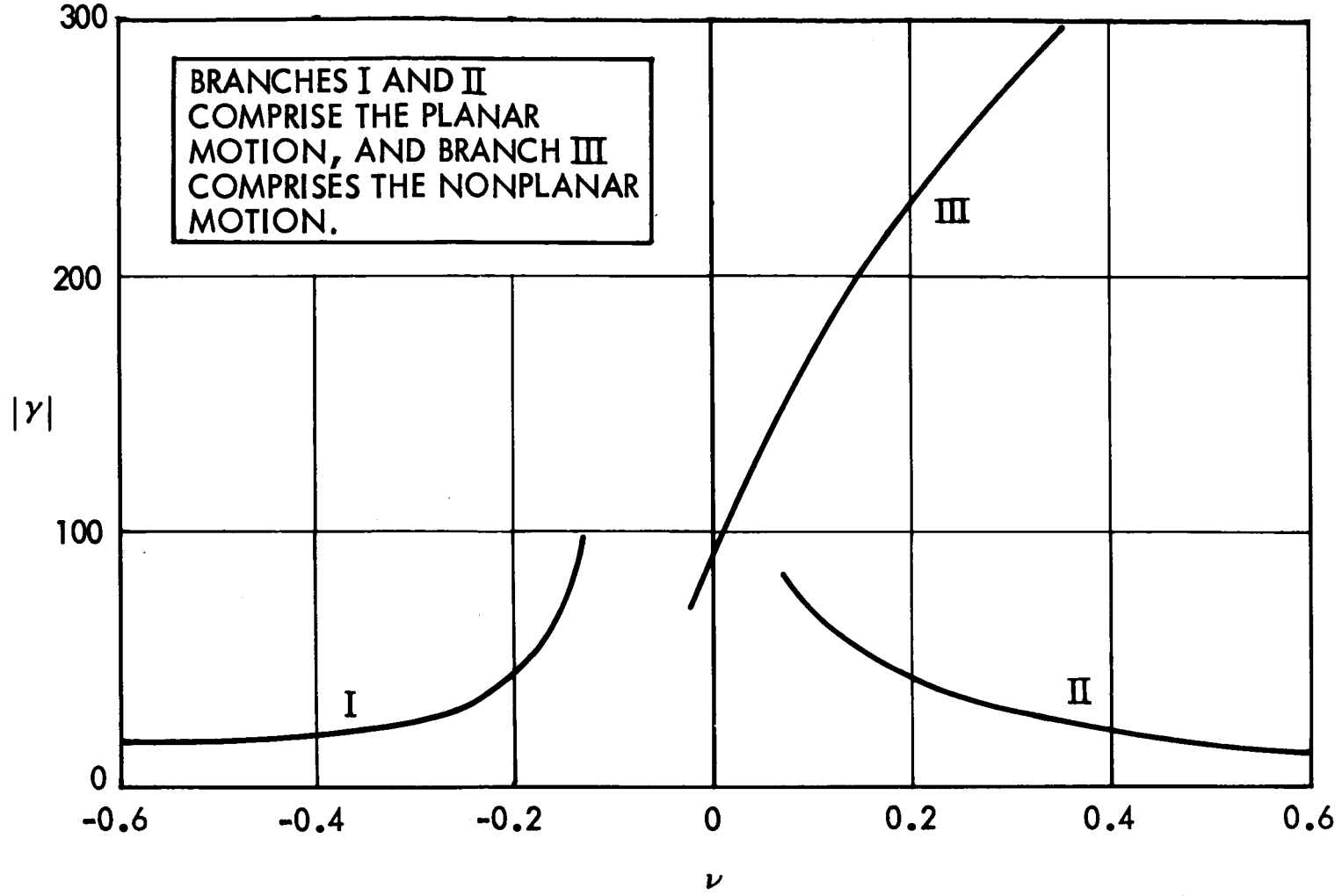

Figure 6. Stable Branches for Forced Oscillations of a Cylindrical Tank of Fluid

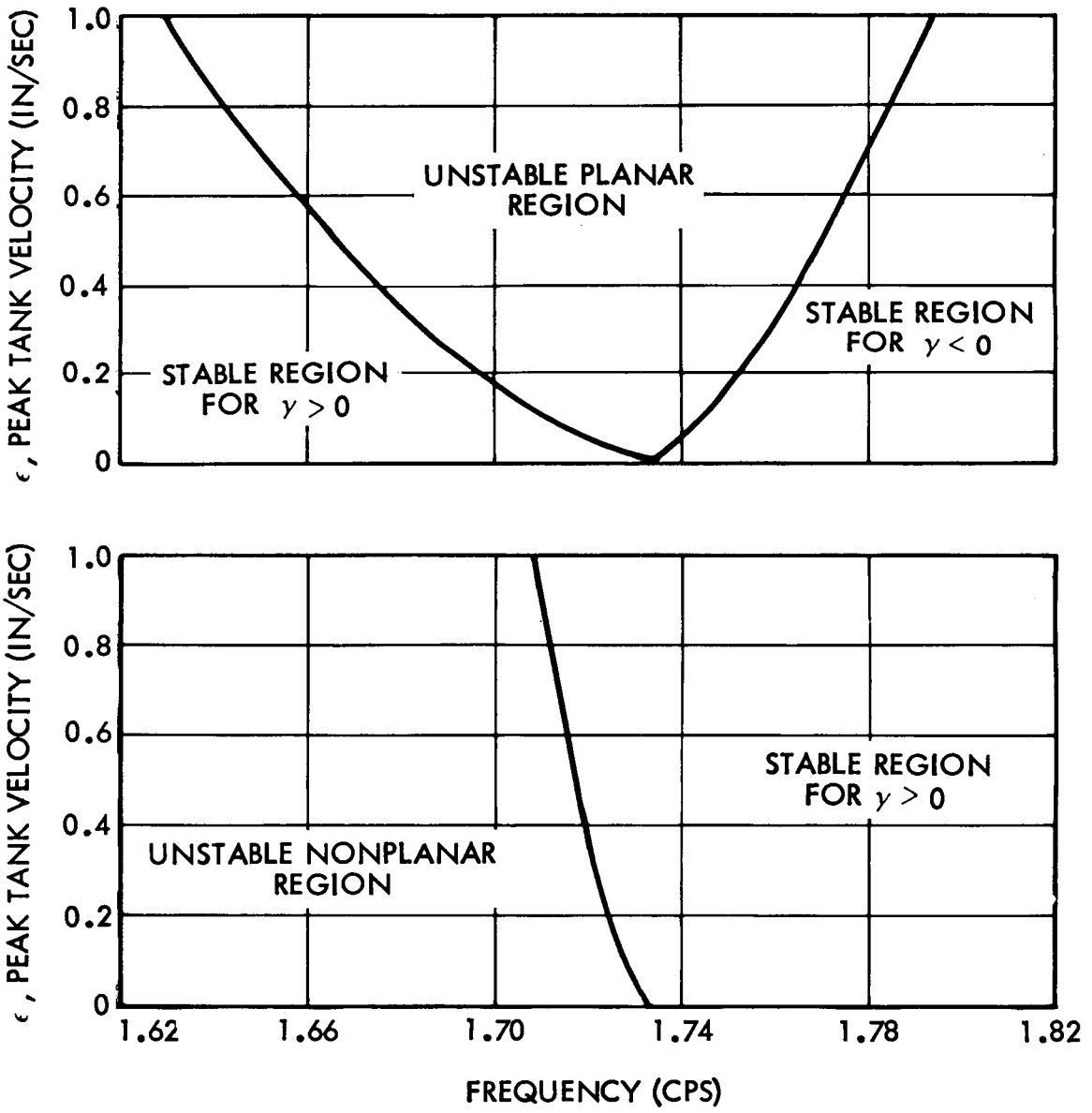

Figure 7. Unstable Regions for Planar and Nonplanar Harmonic Motions

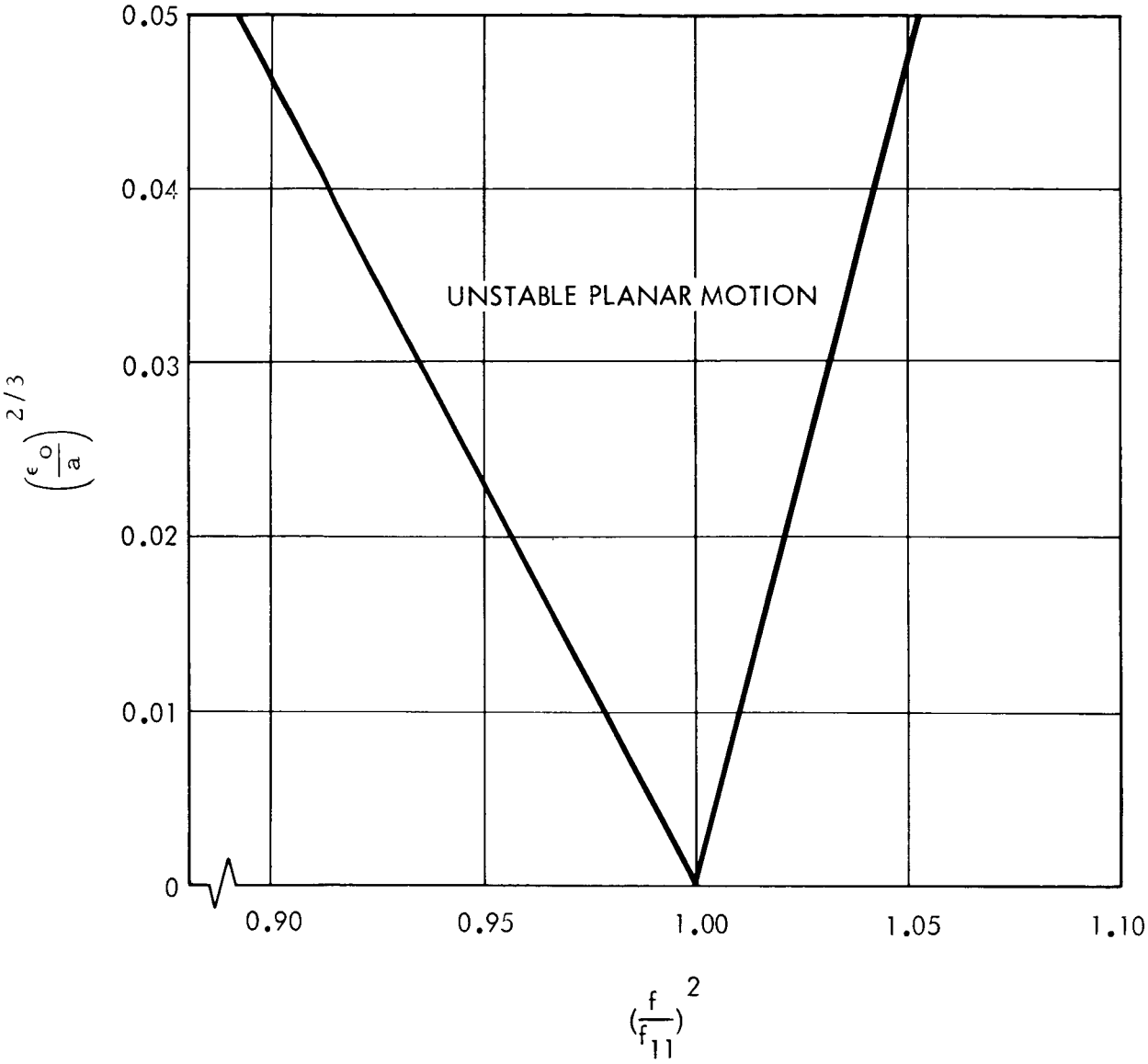

Figure 8. Planar Motion Instability Region as a Function of Nondimensional Driving Frequency and Amplitude

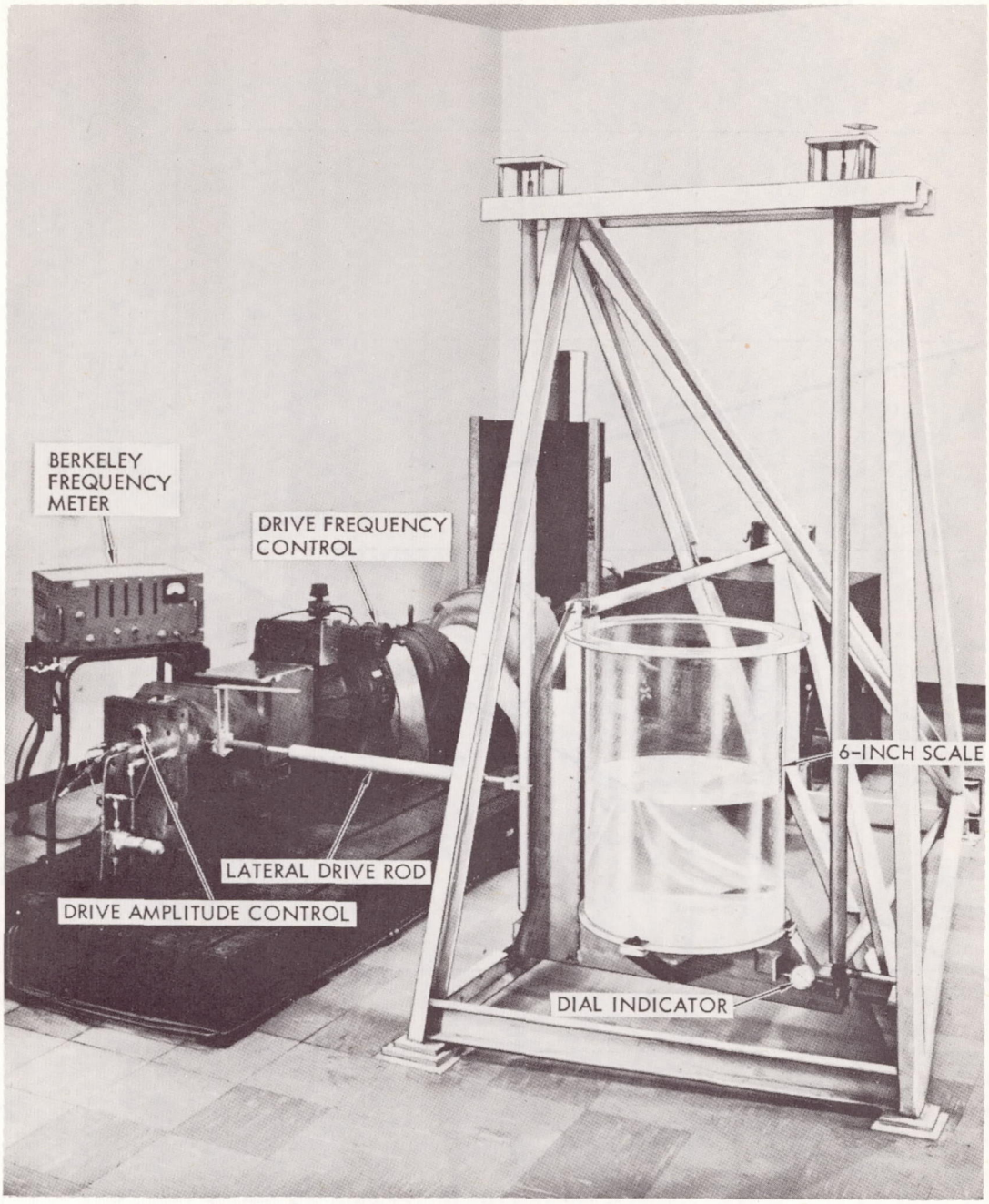

Figure 9. Slosh Test Facility With One-Degree-of-Freedom Tank Platform Laterally Oscillated with Scoth-Yoke Sinusoidal-Drive Mechanism

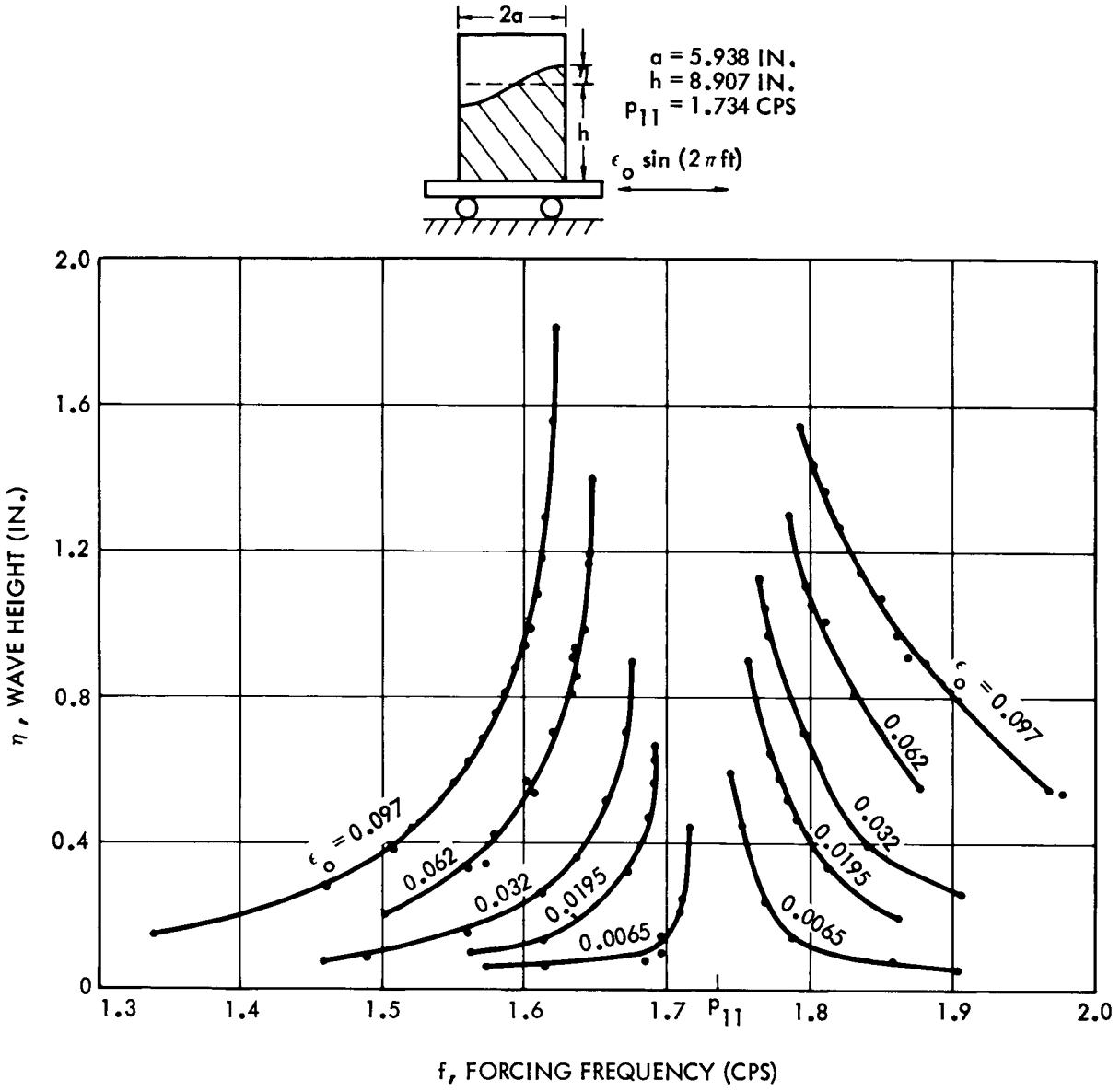

Figure 10. Wave Height Test Data for Planar Motion

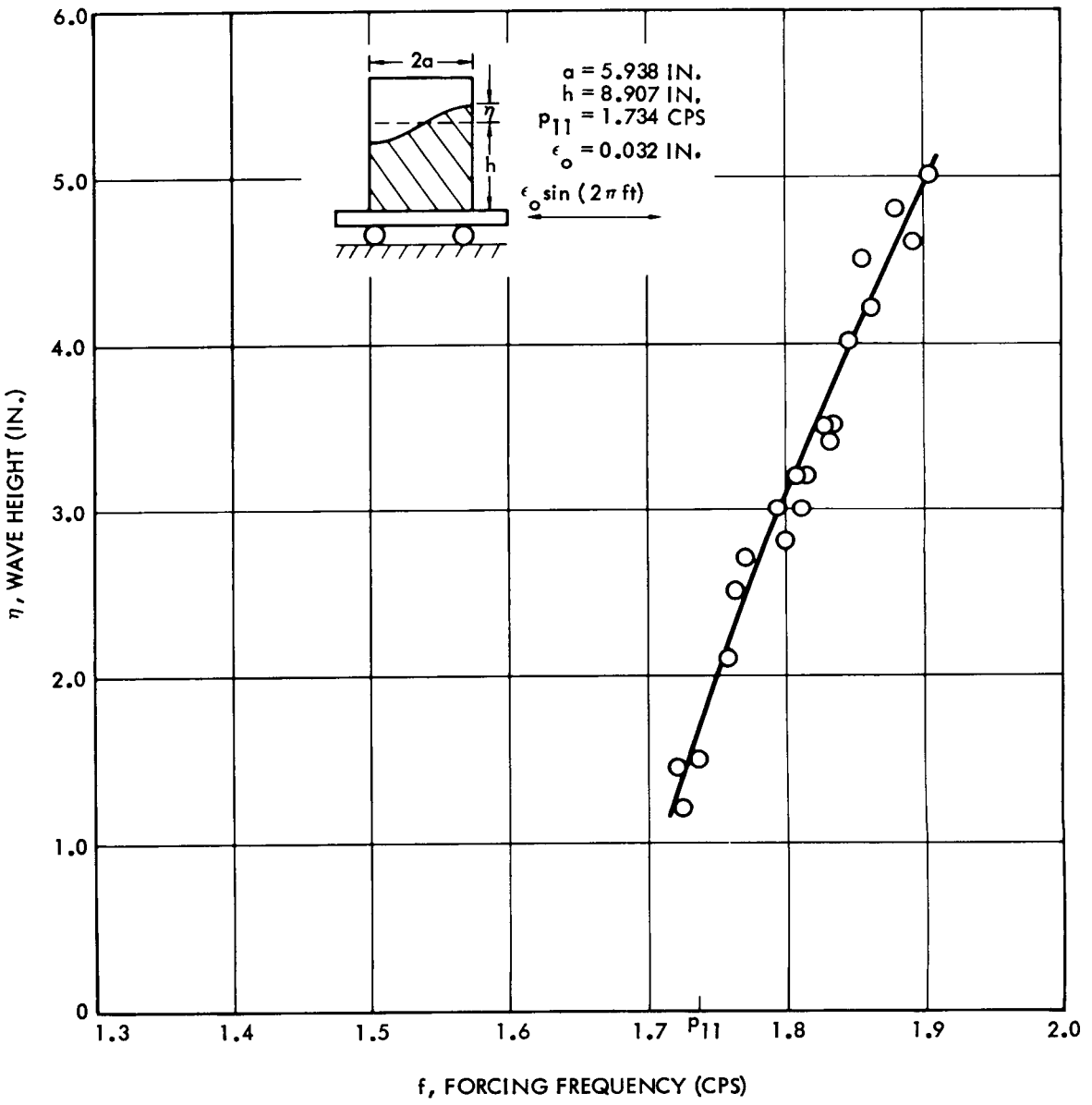

Figure 11. Wave Height Test Data for Nonplanar Motion

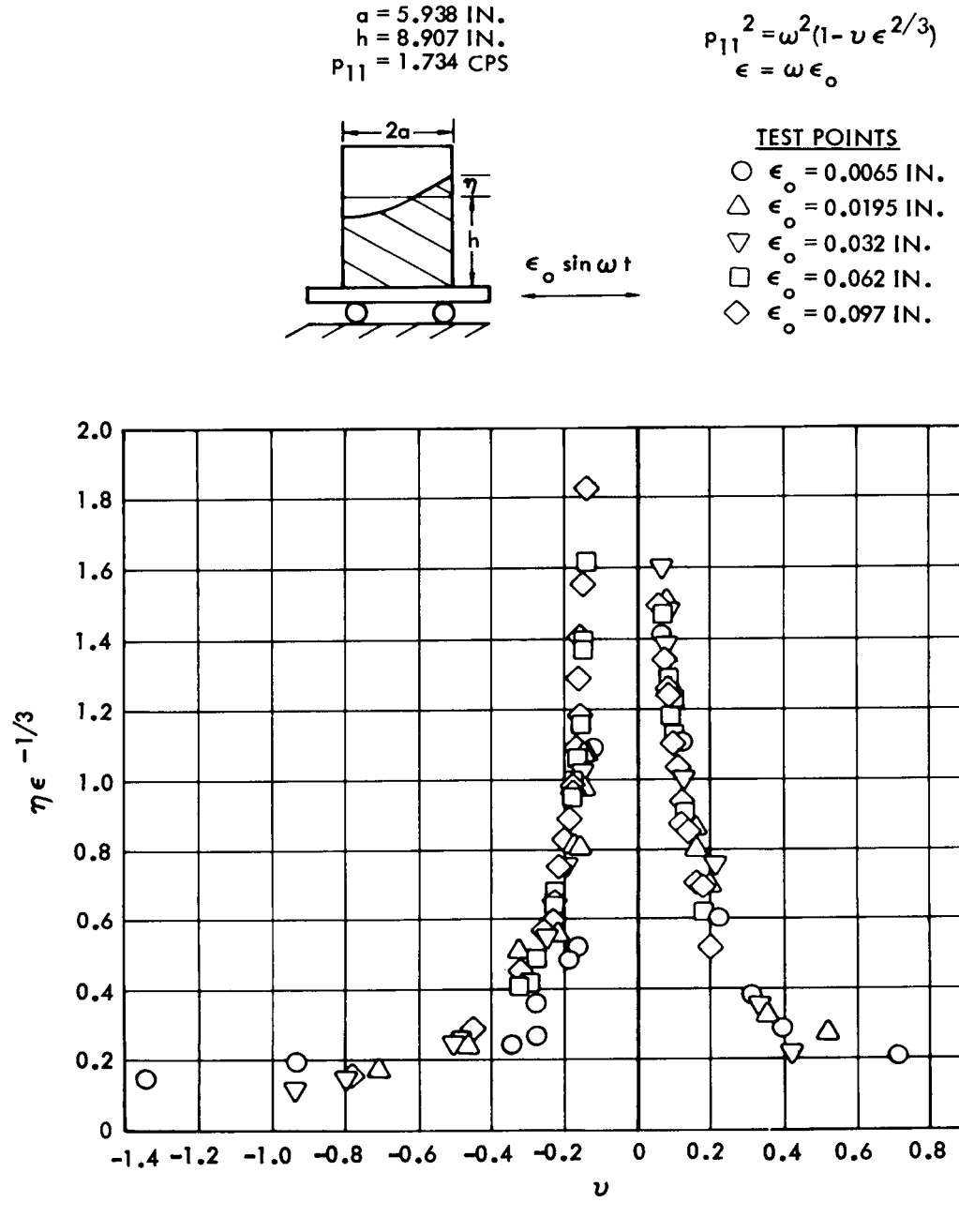

Figure 12. Scaled Wave Height Test Data for Planar Motion

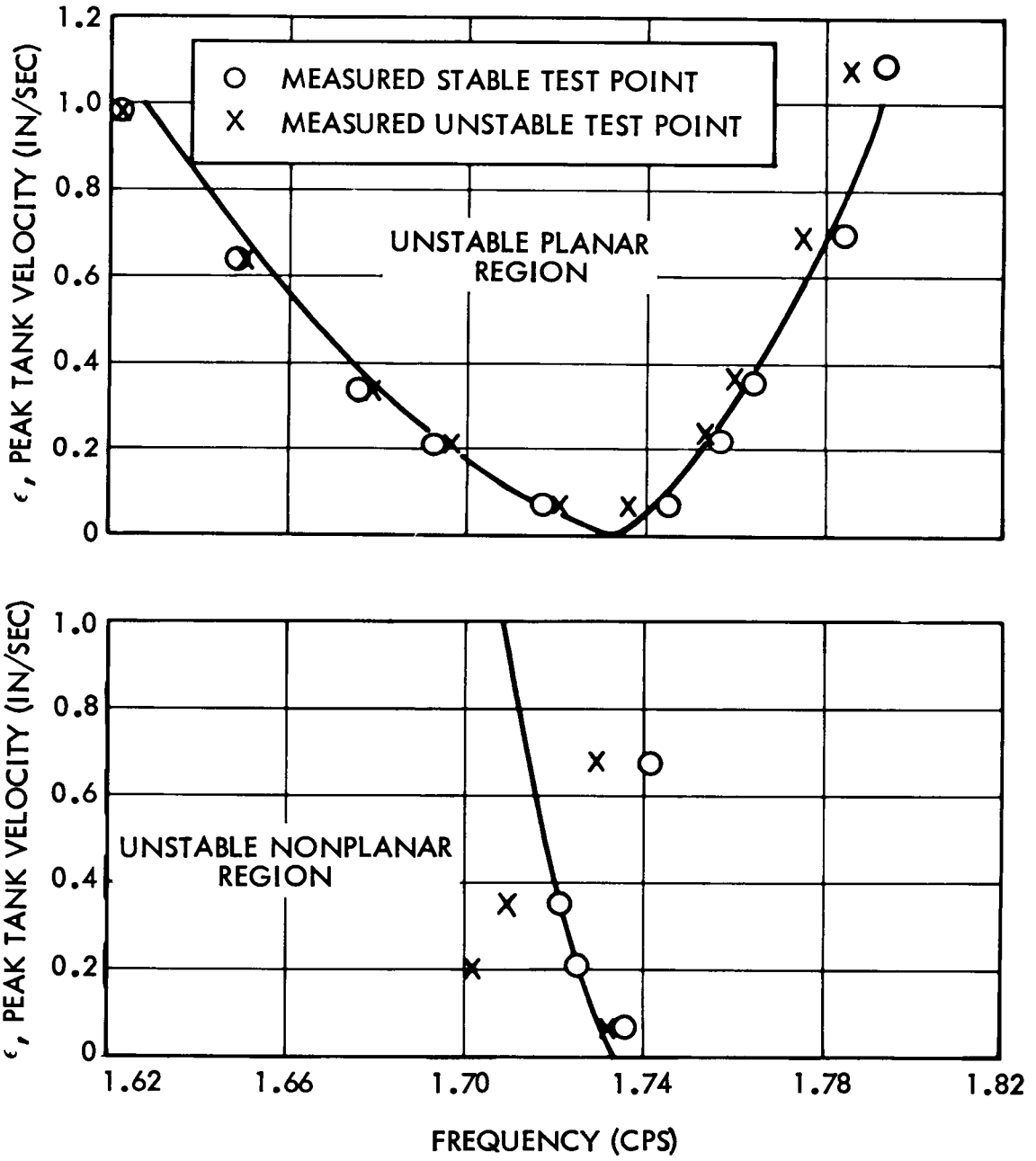

Figure 13. Comparison of Theoretical and Experimental Planar and Nonplanar Instability Regions